

**UNIVERSITY OF GAZIANTEP
GRADUATE SCHOOL OF
NATURAL & APPLIED SCIENCES**

**INVESTIGATION OF FLOW CHARACTERISTICS THROUGH
BOX SHAPE CULVERT COMBINED WITH BROAD CRESTED
WEIR**

**M.Sc. THESIS
IN
CIVIL ENGINEERING**

**BY
MOHAMMED HAMAD
JANUARY 2013**

**Investigation of Flow Characteristics through Box Shape Culvert
Combined With Broad Crested Weir**

**M.Sc. Thesis
In
Civil Engineering
University of Gaziantep**

**Supervisor
Assoc. Prof. Dr. Aytac Güven
Co-supervisor
Assist. Prof. Shahin Sabir**

**By
Mohammed HAMAD
January 2013**

© 2013 [Mohammed HAMAD]

T.C.
UNIVERSITY OF GAZİANTEP
GRADUATE SCHOOL OF
NATURAL & APPLIED SCIENCES
CIVIL ENGINEERING DEPARTMENT

Name of the thesis: Investigation of Flow Characteristics through Box Shape
Culvert Combined with Broad Crested Weir

Name of the student: Mohammed HAMMED

Exam date: January, 2013


Approval of the Graduate School of Natural and Applied Sciences


Assoc. Prof. Dr. Metin BEDİR
Director

I certify that this thesis satisfies all the requirements as a thesis for the degree of
Master of Science.


Prof. Dr. Mustafa GÜNAL
Head of Department

This is to certify that we have read this thesis and that in our opinion it is fully
adequate, in scope and quality, as a thesis for the degree of Master of Science.


Assoc. Prof. Dr. Aytaç Güven

Supervisor

Examining Committee Members

Signature

Prof. Dr. Mustafa GÜNAL

Assoc. Prof. Dr. Aytaç GÜVEN

Assist. Prof. Dr. Hüsnü UĞUR





I hereby declare that all information in this document has been obtained and presented in accordance with academic rules and ethical conduct. I also declare that, as required by these rules and conduct, I have fully cited and referenced all material and results that are not original to this work.

Mohammed HAMAD

ABSTRACT

INVESTIGATION OF FLOW CHARACTERISTICS THROUGH BOX SHAPE CULVERT COMBINED WITH BROAD CRESTED WEIR

HAMAD, MOHAMMED

MSc Thesis in Civil Engineering

Supervisor: Assoc. Prof.Dr.Aytaç Güven; Co-supervisor: Shahin Sabir

January 2013, 76 Pages

This research investigates the hydraulic characteristics of simultaneous flow over broad crested weir and through box culverts experimentally, as well as identifying the effect of parameters, such as upstream head, length, culvert inlet shape, culvert internal dimension, weir crest height, weir side slope angle, weir width, on the performance of combined structures .By this, it is aimed observe the variation in the discharge coefficient (C_d) of the combined structure. Finally, the equations are derived to estimate the flow rate through the combined structure. For this purpose twelve (12) glass models of combined broad crested weir and box culvert were manufactured and tested in a laboratory flume. These models were divided into four groups based on the box culvert dimensions; each group consisting of three models. The experiments were performed in three stages, flow through the box culvert, flow over the broad crested weir, and flow through both the box culvert, and over the broad crested weir simultaneously. Dimensional analysis was performed to obtain the dimensionless parameters that the discharge coefficient depends on. Discharge coefficient prediction equations as a function of the dimensionless terms were developed using (a) multivariable linear regression and (b) multivariable power regression.

Key Words: Culverts, broad-crested weirs, combined structures, discharge coefficient.

ÖZET

BİRLEŞİK KUTU TİPİ MENFEZ-GENİŞ TEPELİ SAVAK YAPISINDA OLUŞAN AKIM KARAKTERİSTİKLERİNİN İNCELENMESİ

HAMAD, MOHAMMED

Yüksek lisans Tezi, İnşaat Mühendisliği

Danışman: Doç. Dr. Aytaç Güven, Yardımcı Danışman: Şahin Sabir

Ocak 2013, 76 Sayfa

Bu çalışma, birleşik kutu tipi menfez-Geniş tepeli savak yapısında oluşan akım karakteristiklerini deneysel olarak araştırmaktadır. Menba su yüksekliği, menfez uzunluğu, menfez iç geometrisi, menfez iç yarıçapı, savak tepe yüksekliği, savak yan eğim açısı, savak genişliği gibi en etkili parametrelerin yapının performansı üzerindeki etkileri incelenmiştir. Bununla birlikte, yapının debi katsayısı (C_d)'nın değişiminin irdelenmesi hedeflenmektedir. Son olarak, yapının debisini tahmin eden denklemler elde edilmiştir. Bu amaçla, yapının 12 cam-modeli geliştirilerek bir laboratuvar kanalı içinde modellemeler yapılmıştır. Bu modeller, menfez boyutlarına bağlı olarak 4 gruba ayrılmıştır, her grupta 3 farklı model bulunmaktadır. Deneysel çalışma üç aşamada gerçekleştirilmiştir: sadece menfez akımı, sadece geniş tepeli savak akımı, ve birleşik menfez-geniş tepeli savak akımı. Fiziksel değişkenler üzerinde boyut analizi yapılarak debi katsayısı üzerinde en etkili boyutsuz parametreler elde edilmiştir. Elde edilen bu boyutsuz parametrelere bağlı olarak, debi katsayısını tahmin eden denklemler (i) çoklu lineer regresyon ve (ii) çoklu üstel regresyon analizleri kullanılarak elde edilmiştir.

Anahtar Kelimeler: Kutu menfe, geniş tepeli savaklar, birleşik yapılar, debi katsayısı.

Presented to my father, my wife, my family and all of my friends

ACKNOWLEDGMENTS

First and foremost, I would like to express my sincere gratitude to my supervisor, Assoc. Prof. Dr. Aytaç Güven, who has supported me and encouraged me in every point of this dissertation and his guidance helped me in all the time of research and writing of this thesis.

I wish express my sincere appreciation and profound gratitude to co-supervisor, Assist. Prof. Shahin Sabir Ahmed, this person has provided me with necessary assistance, suggestion, and immense knowledge that I will never forget.

This thesis may not have been possible without the guidance and the help of the many people. It is a pleasure to thank those who really supported me and have done very hard work to complete this writing.

Lastly, I offer my regards and blessings to my family and all of those who supported me in any respect during study, research and application in the process of this work.

LIST OF CONTENTS

ABSTRACT	vi
ÖZET	vii
ACKNOWLEDGMENTS	viii
LIST OF CONTENTS	ix
LIST OF FIGURES	xii
LIST OF TABLES	xiv
LIST OF SYMBOLS	xv
CHAPTER 1	1
INTRODUCTION	1
1.1 General	1
1.2 Culverts	3
1.3 Weirs	6
1.4 Broad-Crest Weirs	6
1.4.1 Classification of Broad Crest Weirs	7
1.5 Objective of Study	8
CHAPTER 2	9
LITERATURE REVIEW	9
2.1 General	9
2.2 Review of Works Carried on Culverts	9
2.3 Reviews of Works Carried on Broad Crested Weir	11
CHAPTER 3	16

THEOROTICAL ANALYSIS	16
3.1 General.....	16
3.2 Flow Thought the Culvert	16
3.3 Flow over the BroadCrested Weir.....	19
3.4 Combined Structure Flow	22
3.5 Dimensional Analysis	23
CHAPTER 4	28
EXPERIMENTAL SETUP AND METHODOLOGY	28
4.1 General.....	28
4.2 Experimental Setup.....	28
4.2.1 The Flume	28
4.2.2 The Overhead Tank.....	31
4.2.3 The V-notch weir.....	31
4.2.4 The Measuring Tank	32
4.2.5 Point Gages for Depth Measurement.....	35
4.3 Construction of the Models	35
4.4 Testing Program.....	37
CHAPTER 5	38
DATA ANALYSIS AND DISCUSSION OF RESULTS	38
5.1 General.....	38
5.2 Head - Discharge Relations	38
5.3 Effect of Weir Height (P).....	42
5.4 Effect of the Side Slope (θ)	44
5.5 Effect of the Culvert Dimension (D).....	45
5.6 Correlations for Discharge Coefficient (Cd).....	47

5.6.1 Discharge Coefficient Regressions for the Culvert	47
5.6.2 Discharge Coefficient (Cd) for the Broad Crested Weir	48
5.6.3 Discharge Coefficient (Cd) for the Combined Structure	49
CHAPTER 6	56
CONCLUSIONS AND RECOMMENDATIONS.....	56
6.1 General.....	56
6.2 Conclusions	56
6.3 Recommendations for further Investigations.....	57
REFERENCES.....	58
APPENDICES	60
Appendix A: Sample of Calculation	61
Appendix B: Measured Data and Calculated Results.	63

LIST OF FIGURES

Figure 1.1 Sketch of roadway culverts during normal stream flow	2
Figure 1.2 Sketch of roadway culverts during floods	2
Figure 1.3 Types of culvert flow(Chow 1959).....	5
Figure 1.4 Broad crested weir (Bos, 1976)	6
Figure 1.5 Flow types of broad crested weir.....	7
Figure 2.1 Profile of the flume used by Ehab A. Meselhe and Kirby Hebert(2003), showing locations of the water level sensors.	10
Figure 2.2 Steady free flow experiment (Upstream head versus discharge) tests by Ehab A. Meselhe and Kirby Hebert(2003)	11
Figure 2.3 Definition sketch for simultaneous flow through box culvert and over contracted broad crested weir tested by Abdul Azim M. Negm	14
Figure 3.1Culvert flow (R. E. Featherstone & C. Nalluri)	16
Figure 3.2 Flow over broad crested weir (M. HanifChaudhry).	20
Figure 3.3 broad crested weir with trapezoidal cross section	21
Figure 3.4 combined structure flow(M. HanifChaudhry)	23
Figure 3.5 Definition of symbolism for the combined structure.....	24
Figure 4.1 The Flume use din the study	29
Figure 4.2 The Flume used in the study.....	30
Figure 4.3 The Overhead tank and the V-notch weir used in the study.....	31
Figure 4.4 Details of the V- notch weir.....	32
Figure 4.5 The measuring tank manufactured for the calibration of the V-notch weir	33

Figure 4.6 Calibration curve of the V- notch weir	34
Figure 4.7 Point gages with its carriage	35
Figure 4.8 One of the models	36
Figure 4.9 Definition of symbolism of the models	36
Figure 5.1 Head Discharge Relations for Models 1-4.....	39
Figure 5.1 Continued, Head Discharge Relations for Models 5-8.....	40
Figure 5.1 Continued, Head Discharge Relations for Models 9-12.....	41
Figure 5.2 Effect of weir height (P) on the Discharge for the BCW	42
Figure 5.2 Continued, Effect of weir height (P) on the Discharge for the BCW.....	43
Figure 5.3 Effect of side slope on the Discharge coefficients for the various models of the combined structure.....	44
Figure 5.4 Head Discharge Coefficient Relations for culvert flow	45
Figure 5.5 Head Discharge Coefficient Relations for culvert flow	46
Figure 5.6 Relation between measured and predicted discharges for the culvert.....	50
Figure 5.7 Relationship between measured and predicted discharges for the BCW .	51
Figure 5.8 Relationship between measured and calculated discharges for the combined structure (a) linear regression (b) power regression.....	52
Figure 5.9 Variation of (Cd) with (H/P), (H/Y), (H/D) and (H/L) for models 1-4....	53
Figure 5.9 Continued, Variation of (Cd) with (H/P), (H/Y), (H/D) and (H/L) for models (5-8).....	54
Figure 5.9 Continued, Variation of (Cd) with (H/P), (H/Y), (H/D) and (H/L) for models 9-12.....	55

LIST OF TABLES

Table 2.1 Characteristics of straight weirs used by Khosrojerdi, and Kavianpour....	13
Table 2.2 Characteristics of curved weirs used by. Khosrojerdi, andKavianpour.....	13
Table 3.1 Types of flow through Culvert (R. E. Featherstone & C. Nalluri).	17
Table 4.1 Calibration Data of the V-notch weir.....	34
Table 5.1 Coefficient of discharge as a function of Y/D for type 5 flow in a culvert with a flared – pipe end section (Bodhaine, 1976).....	45
Table (B-1) Measured and calculated data for combined structure flow.....	63
Table (B-1) Continued	64
Table (B-1) Continued	65
Table (B-1) Continued	66
Table (B-1) Continued	67
Table (B-1) Continued	68
Table (B-2) Measured and calculated data for the Broad Crested Weir flow.....	69
Table (B-2) Continued	70
Table (B-2) Continued	71
Table (B-2) Continued	72
Table (B-2) Continued	73
Table (B-2) Continued	74
Table (B-3) Measured and calculated data for the Culvert flow.....	75
Table (B-3) Continued	76

LIST OFSYMBOLS

A	Cross sectional Area
b	width of the weir
BCW	Broad Crested Weir
C_d	Discharge Coefficient
D	Culvert internal diameter
DS	Downstream
f	Darcy-Weisbach friction factor (head loss coefficient)
g	Gravitational acceleration
h	Head of water above the weir crest
h_v	Head of water above the V-notch the weir crest.
h_f	Frictional head loss.
H	Total head of water above weir crest
L	Length
P	Pressure
q	Discharge per unit width
Q	Discharge
Q_t	Total discharge
Q_w	Discharge over the weir.
Q_c	Discharge through culvert.
S_o	Longitudinal slope of the culvert.
TEL	Total energy line.

US	Upstream.
v_D	Average velocity in culvert.
v_o	Average upstream approach velocity.
v_c	Average critical flow velocity.
We	Weber number.
y_o	Uniform water depth in the channel.
y_c	Depth of flow at critical section.
y_t	Tail water depth.
Y	Upstream total head above the culvert bottom.
Z	Elevation head.
π	Dimensional group.
α	Coriolis coefficient.
γ	Weight density of water.
ρ	Mass density of water.
σ	Surface tension of water
μ	Dynamic viscosity of water.
θ	Angle between crest of the weir with the sides.

CHAPTER 1

INTRODUCTION

1.1 General

Streams and rivers are formed by runoff flowing towards low elevation areas. In mountainous places rainfall and precipitated ice thawing are the main source of runoff. In (Iraq) within water year precipitation is confined between winter and spring seasons while for the rest months (Jun to the end of September) there is no rainfall. Therefore several streams in the region have flow only in few months throughout the water year, while they are dry for most time in a year.

In general streams can be classified into the following types [1]:

- a. Perennial: water flows in the well defined channel at least (90% of the time).
- b. Intermittent: flow generally occurs only during the wet season (50% of the time or less).
- c. Ephemeral: flow generally occurs in a short time after extreme storms.

According to the above classification several streams in the region can be classified within the third type (Ephemeral). When seasonal streams which have flood for few hours, cross a road way it needs to be provided with a passage for vehicles and persons. If only culvert cannot convey all of the incoming water at large flows or peak of floods, the designer will have the following two possible alternatives:

- i. Design and construction of a bridge with dimensions capable for maximum discharge of the stream of return period equal to the economical life of the construction project, since bridges are high level crossing structures which are expensive for wide rivers, in this case it needs more time and cost to construct it.

Or

- ii. Design and construction of culverts for normal stream flow (Fig 1.1) and allow the water to flow over the road during peak flood which occur few times in the year or rarely during the economical life (usually 25 years) of the culvert (Fig 1.2). This choice needs construction time and cost less than former, but traffic may be restricted during the flood events.

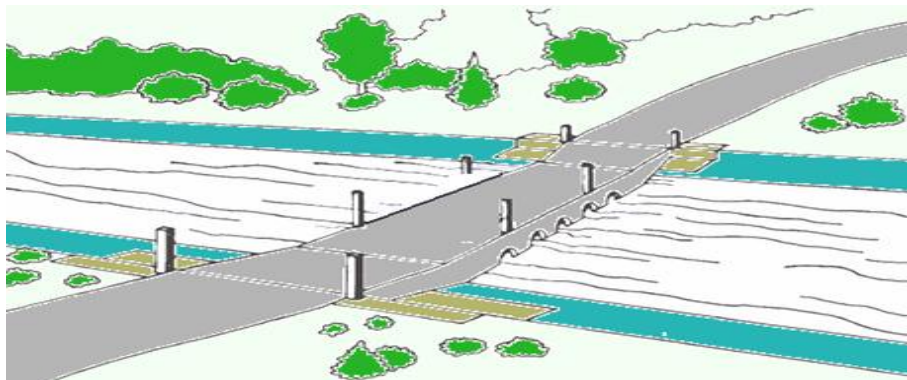


Figure 1.1 Sketch of roadway culverts during normal stream flow

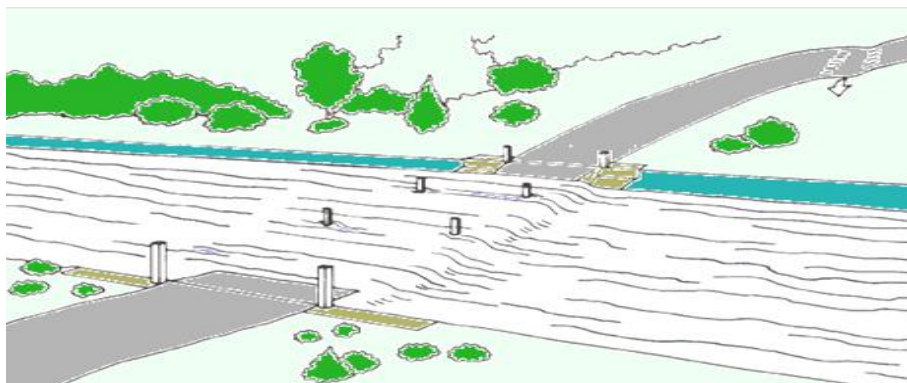


Figure 1.2 Sketch of roadway culverts during floods

The main operational differences between culverts and bridges may be described in terms of [2]:

- Economics.
- Hydraulics.
- Structural aspects.
- Maintenance attention requirements

Economically, the initial and operating costs of culverts are considerably less than that of bridges.

Roadway overtopping will begin when the headwater rises to the elevation of the roadway. The overtopping will usually occur at the lowest point of the sag vertical curve on the roadway. The overtopping flow will be similar to flow over a broad crested weir.

For the purpose of studying flow characteristics over submerged culverts it is essential to describe both culverts and broad crested weirs in detail individually

1.2 Culverts

Culverts are important and common crossing hydraulic structures. Understanding the variety of flow regimes through culverts is necessary to evaluate their hydraulic performance in flood studies, operation of irrigation systems, and environmental studies, during rainstorms overtopping of roadways may occur. Combined broad crested weir and culvert flow would result, and the discharge carrying capacity of the culvert barrels may be affected [3].

A short passage way for flow under a highway, railroad, or other embankment is referred to as a culvert. The culvert may be circular, rectangular, arch, or elliptical in shape. A rectangular culvert is referred to as a box culvert [4].

Although a culvert is a simple hydraulic structure, the computation of flow conditions through it may be somewhat complex. This is because several different flow conditions are possible and these conditions depend upon several parameters. The culvert may flow full, or partially full throughout its length, or in part of the length. The control may be at the upstream end (called inlet control) or it may be at the downstream end (called outlet control). Depending upon the head and tailwater levels, the control may shift from the inlet to the outlet and vice versa as these water levels change.

A variety of flow types can occur in a culvert, depending on the upstream and downstream conditions, the inlet geometry, and the conduit characteristics. A culvert may flow full, partially full (in subcritical or supercritical flow conditions), or a combination of both. Partially full flow can be subcritical or supercritical. [5]

(Chow 1959) [6] Defined six flow types through culverts based on the relative heights of the upstream head and tailwaters, these six flow types are summarized in (Fig 1.3)

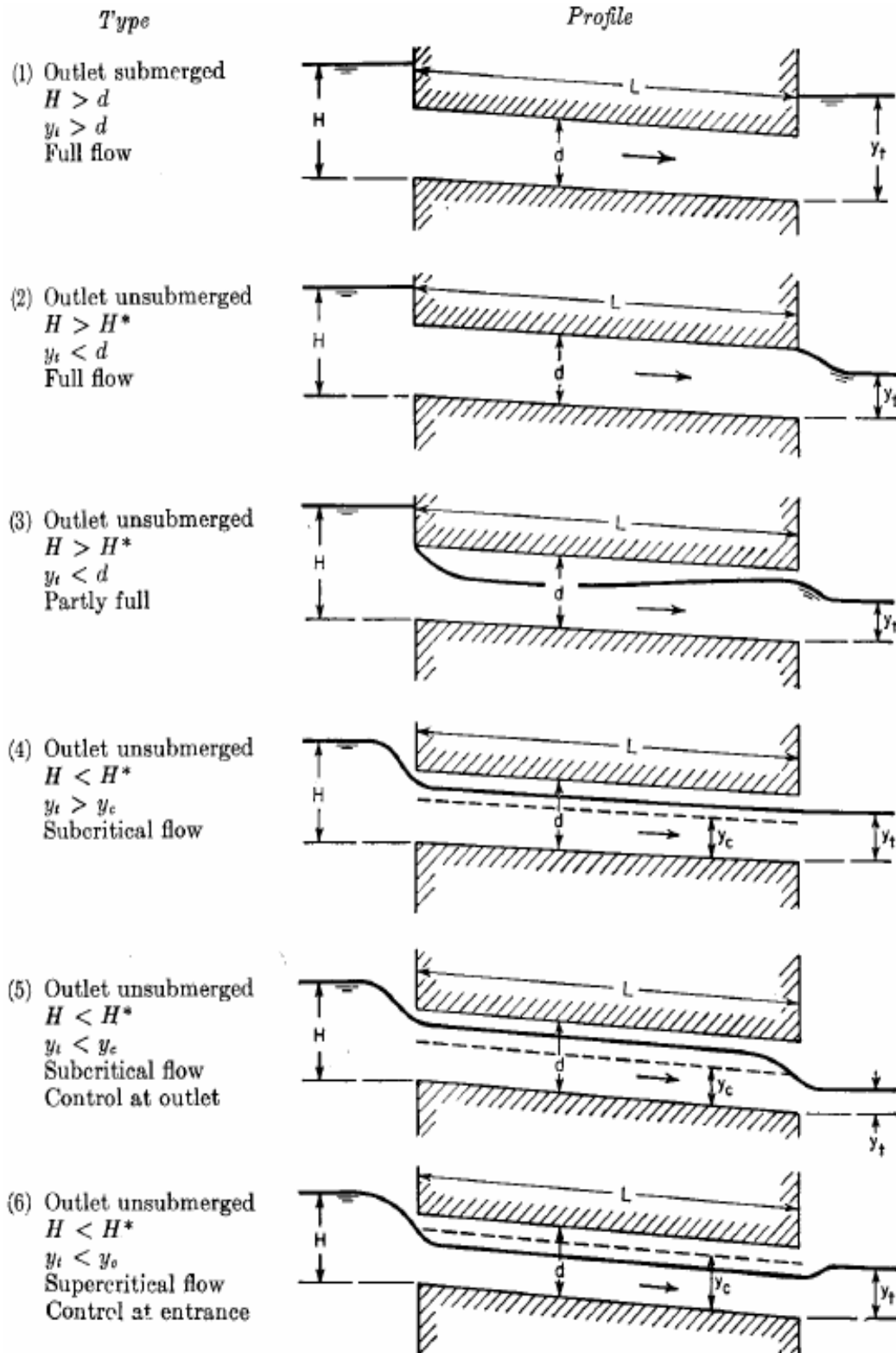


Figure 1.3 Types of culvert flow(Chow 1959)

$H^* = (1.2 \text{ to } 1.5) d$, depending on the entrance geometry of the culvert

1.3 Weirs

The weir is an obstruction constructed across a river or stream for the purpose of rising water surface or for water flow measurement. Weirs are extensively used in hydraulic structures to control the flow depth and discharge. They are classified in two branches of sharp crested and broad crested weirs. The crest of the weirs may also be straight or curved.

1.4 Broad-Crest Weirs

A broad crested weir is a structure with a horizontal crest above which the fluid pressure may be considered hydrostatic. If such a situation is to exist, then with reference to (Fig 1.4) the following inequality must be satisfied, [7,8].

$$0.08 \leq \frac{H}{L} \leq 0.5 \quad (1.1)$$

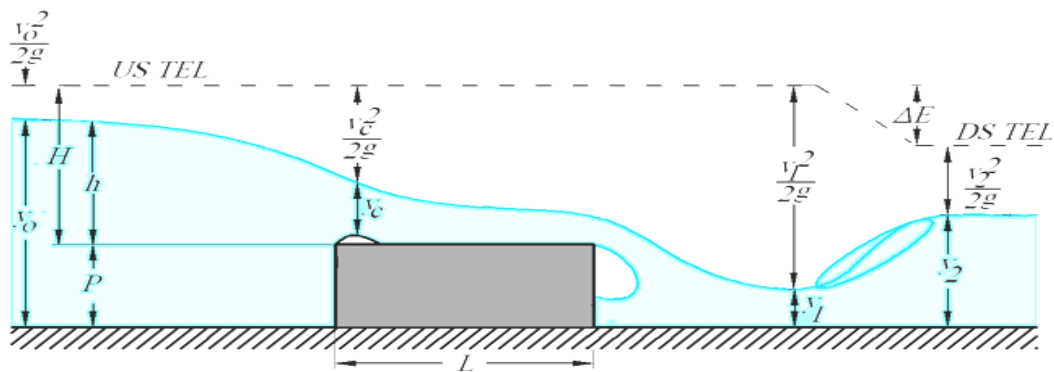


Figure 1.4 Broad crested weir (Bos, 1976)

If the upstream corner of the weir is sharp then the flow will separate and then reattach enclosing a separation bubble. But if the upstream corner is rounded this separation bubble will not exist.

1.4.1 Classification of Broad Crest Weirs

Based on the value of (h/L) the flow over a broad crested weir with an upstream sharp corner is classified as follows [9].

1. $(h/L) \leq 0.1$: In this range the critical flow control section is at the downstream end of the weir and the resistance of the weir surface plays as important role in determining the value of (C_d) (Fig 1.5a) this kind of weir, termed as long-crested weir, finds limited use as a reliable flow measuring device.
2. $0.1 \leq (h/L) \leq 0.35$: The critical depth control occurs near the upstream end of the weir and the discharge coefficient varies slowly with (h/L) in this range (Fig 1.5b) this kind can be called a true broad crested weir.
3. $0.35 \leq (h/L) \leq$ about 1.5: The water surface profile will be curvilinear all over the weir. The control section will be at the upstream end (Fig 1.5c) the weirs of this kind can be termed as a narrow crested weir. The upper limit of this range depends upon the value of (h/P) .
4. $(h/L) >$ About 1.5: The flow separates at the upstream corner and jumps clear across the weir crest. The flow surface is highly curved (Fig 1.5d), and the weir can be classified as sharp crested

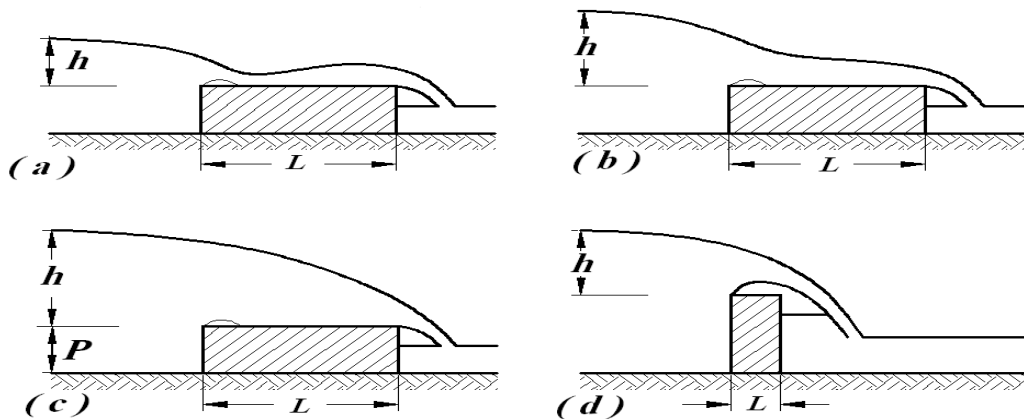


Figure 1.5 Flow types of broad crested weir

1.5 Objective of Study

The main objective of this research is to study relations between variables (P , D , θ , h) of the combined structure. The procedures to accomplish this objective are as follows:

1. Studying the head discharge relations for each structure separately (weir, culvert and combined structure).
2. Studying the effect of weir crest height (P), weir side slope angle (θ) and internal box culvert dimension (D) on the discharge coefficient (C_d).
3. Finding experimental rational equations for the discharge coefficient (C_d)
4. For each flow condition (weir, culvert and combined structure).

CHAPTER 2

LITERATURE REVIEW

2.1 General

Articles of this chapter will present a brief review of significant experimental studies (obtained) associated with the following subjects:

1. Culverts.
2. Broad Crested Weir.
3. Simultaneous Flow over and under Hydraulic Structures

2.2 Review of Works Carried on Culverts

Culverts have been utilized for thousands of years as a means to transmit water under walkways and roadways.

Several researchers performed model tests on scour downstream of culverts and the combined results suggest the following Formulas [10,11]:

- Scour depth below bed level, (y_s):

$$y_s = 0.65 D \left(\frac{U_o}{U_{*c}} \right)^{\frac{1}{3}} \quad (2.1)$$

- Scour width, (B_s):

$$B_s = 7.5 D Fr^{2/3} \quad (2.2)$$

- Scour length,

$$L_s = 15 D Fr^{2/3} \quad (2.3)$$

where: U_o : flow velocity at exit; U_{*c} : shields critical shear velocity, $U_{*c} = (\tau_c/\rho)^{1/2}$; τ_c :

critical shear stress; (ρ): mass density of water ;(D): culvert height ;(Fr): froude number; $Fr=U_o / (gD)^{1/2}$.

Ehab A. Meselhe and Kirby Hebert (2003)[3], presented a study to simulate flow through culverts for the different flow conditions with and without weir overtopping.

The culvert configurations used was a low weir (overall height of 154 mm above the flume floor) with two (76.2) mm diameter round culverts with inlet inverts of (43.2 mm) and outlet inverts of (38.1 mm) for a slope of (0.01333) over the (0.381 m) length of the culvert. The two culverts were placed symmetrically about the centreline of the structure with their centres at (76.2 mm) from the overall structure centreline as shown in Figure 2.1.

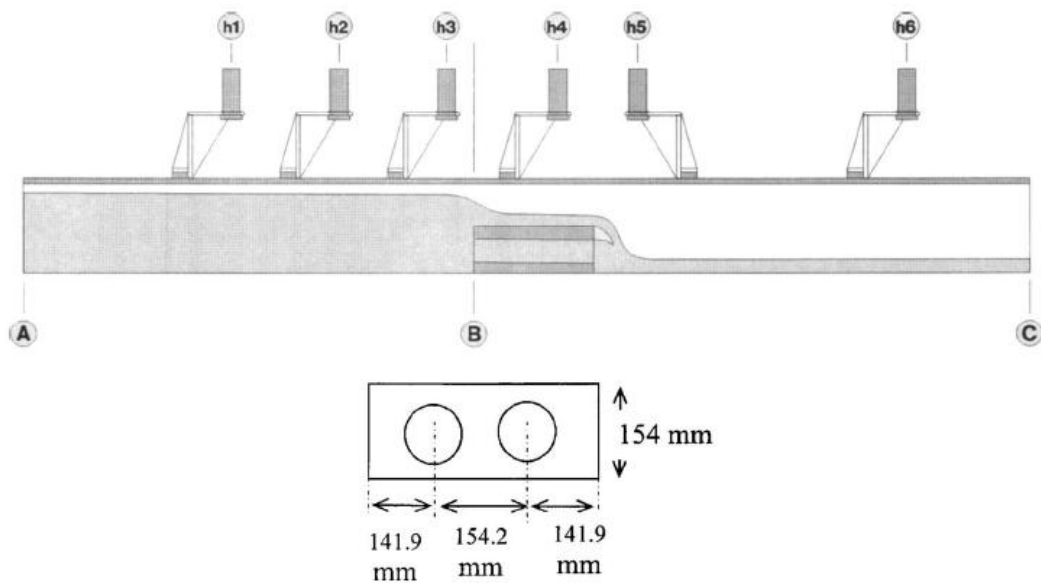


Figure 2.1 Profile of the flume used by Ehab A. Meselhe and Kirby Hebert(2003), showing locations of the water level sensors.

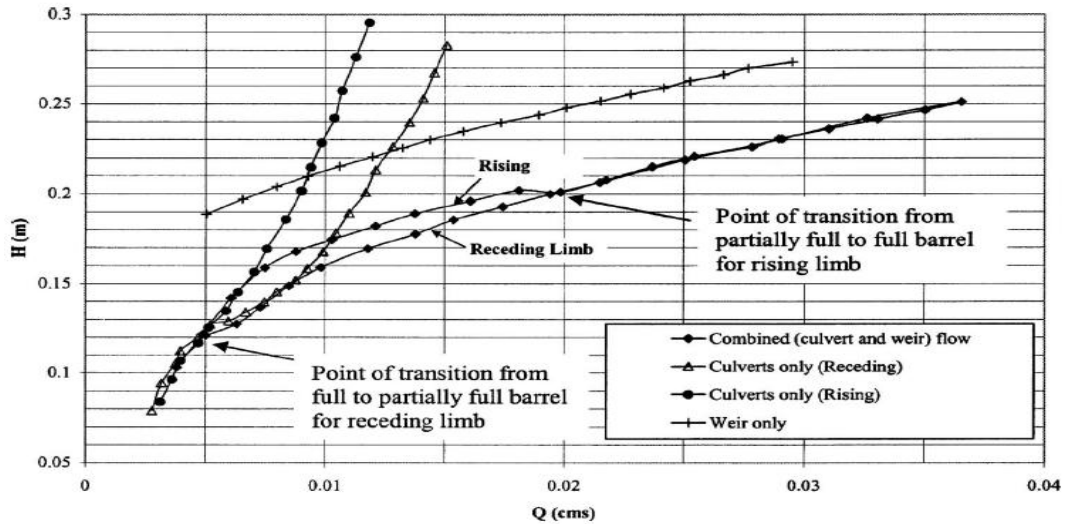


Figure 2.2 Steady free flow experiment (Upstream head versus discharge) tests by Ehab A. Meselhe and Kirby Hebert(2003)

2.3 Reviews of Works Carried on Broad Crested Weir

In engineering literature, the term “weir” is commonly applied to structures that divert the flow or control the level of a waterway. The study of weirs has attracted the attention of many investigators since the 18th century, the general equation of discharge for rectangular weirs was first proposed by Poleni (1717) [12,13] as:

$$Q = \frac{2}{3} C_d \sqrt{2g} L h^{3/2} \quad (2.4)$$

Where: C_d : discharge coefficient of the weir, L : width of the weir; h : head of water on the weir crest; g : the gravitational acceleration.

The effect of the upstream approach velocity was considered by Weisbach (1846), [12], [13], he included the average approach velocity head in the Poleni Eq. (2.4), and then the new equation had developed:

$$Q_{act} = \frac{2}{3} C_d \sqrt{2g} L \left[\left(h + \frac{v_o^2}{2g} \right)^{3/2} - \left(\frac{v_o^2}{2g} \right)^{3/2} \right] \quad (2.5)$$

Where v_o : average approach velocity of the incoming flow upstream the weir.

Francis (1852),[9],[12],[13] studied the effect of side contractions for rectangular weirs, and he concluded the effect of horizontal curvature of the streamlines by developing a new equation:

$$Q_{act} = 1.84 \left[b - 0.1n \left(h + \frac{v_0^2}{2g} \right) \right] \left[\left(h + \frac{v_0^2}{2g} \right)^{\frac{3}{2}} - \left(\frac{v_0^2}{2g} \right)^{\frac{3}{2}} \right] \quad (2.6)$$

Kindsvater, C.E. and R.W (1957). [7], [9], [13] Carter had given a modified version of Eq. (2.4), based on their extensive experimental investigations covering a wide range of variables, as:

$$Q = \frac{2}{3} C_{dc} \sqrt{2g} L_e H_{1e}^{3/2} \quad (2.7)$$

Where: C_{dc} : discharge coefficient of the contracted weir; L_e : effective width of the contracted weir, $L_e = L + K_L$; H_{1e} : effective head of water on the weir, $H_{1e} = H_1 + K_H H_1$: head of water on the weir, L : width of contracted weir, K_H & K_L : are coefficient to account for the combined effect of viscosity and surface tension.

Series of experiments were conducted in Water Research Centre of the Ministry of Energy in Iran. Broad crested weirs with straight and curved shapes were studied by A. Khosrojerdi, M.R. Kavianpour(2002),[18]. The study was based on hydraulic model studies for different wide and curvature of the weir.

They had carried out their experiments in two steps. In the first step, straight weirs were used to determining the discharge coefficient, the position of the critical depth and the water surface profile over the weir.

Second step, experiments were performed with curved weirs. Variation of water surface and discharge were measured to determine the discharge coefficient of the

weirs. Tables (2.1) and (2.2) show details of the weir models tested.

Table 2.1 Characteristics of straight weirs used by Khosrojerdi, and Kavianpour

Weir	R (cm)	L (cm)	H_{max} (cm)	B (cm)	P (cm)
1	5	20	20	75	20
2	5	35	20	75	20
3	5	50	25	75	20

Table 2.2 Characteristics of curved weirs used by. Khosrojerdi, andKavianpour

z	P (cm)	R(cm)	H_{max} (cm)	L (cm)	R (cm)
1	20	High	20	20	5
2	20	122.5	20	20	5
3	20	72.1	20	20	5
4	20	-122.5	20	20	5
5	20	-72.1	20	20	5

* Negative sign represents the convex weirs.

Where: P: weir height;L: width of the weir in the direction of flow; H_{max} : maximum depth of water over the weir; B: length of the weir; R: radius of the weir corners.

Khosrojerdi, and Kavianpour (2002) obtained a new relation for the discharge coefficient for straight broad crested weirs, which is a function of the height (P) and width (L) of the weir and the depth of water over it (h).

The overall results were used to develop a new equation using optimization methods (within 5% error) in the following form:

$$C_d = \left(0.5 + 0.33 \frac{h}{P} + \frac{h}{L} \right)^{0.06} \quad (2.8)$$

Where: h: head of water above the weir.

2.4 Review of the Works Carried on Combined Flow

Abdul Azim M. Negm (2002)[23] had conducted an experimental investigation on simultaneous flow through box culvert and over the broad crested weir. The flow at the culvert outlet is considered as submerged flow. Both the culvert and the broad crested weir (BCW) widths are smaller than the channel width as shown in Figure 2.3.

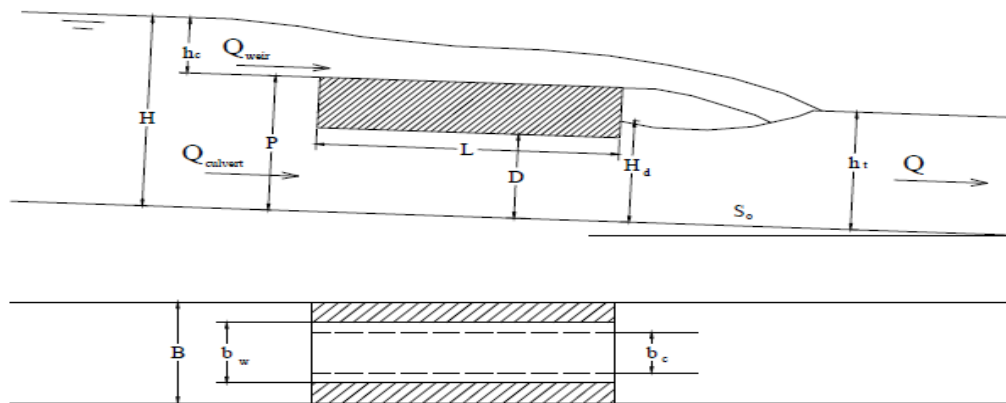


Figure 2.3 Definition sketch for simultaneous flow through box culvert and over contracted broad crested weir tested by Abdul Azim M. Negm

A typical tested model consisted of a contracted broad crested weir combined with one vent box culvert with the same total length from entrance to exit of 40 cm. and 30.5 cm width, and the height of the culvert barrel was kept constant to 6 cm.

The flow at both inlet and outlet of the culvert were submerged and the culvert is flowing full. The approaching discharge to the structure was more than the capacity of the culvert and thus a flow over the weir was expected. The recorded measurements include the flow depth at 40 cm upstream from the culvert inlet and just downstream of the culvert to ensure that the flow over the weir is free. The tailwater depth was recorded several times for each discharge to account for the effect of submergence

$$F = 1.375 - 0.0376S - 0.0675 \frac{H}{D} + 0.0124 \frac{b_w}{D} + 0.0953 \frac{b_c}{D} - 0.3815 \frac{b_w}{b_c} 16.265S_o \quad (2.9)$$

where: F: factor to account for the interaction between the flow over the weir and that through the culvert; S: the submergence ratio (S= tailwater depth / depth of culvert opening); H: the upstream head of water above the canal bed; D: the culvert height; b_w : the width of the weir; b_c : the width of the culvert; S_o : the longitudinal slope of the canal.

The simultaneous discharge over the weir and through the culvert then obtained by equation:

$$\left[\frac{2}{3} C_d C_v b_w \sqrt{\frac{2}{3} g h_w^{3/2}} + C_D A_o \left(\frac{2g(H - h_t)}{1 + (29C_D^2 n^2 L / R_o^{4/3})} \right)^{\frac{1}{2}} \right] \quad (2.10)$$

where: Q: discharge over weir; C_d : coefficient of discharge; C_v : coefficient of velocity; $C_v = (H_o/h_w)^{1.5}$; H_o : total energy head over the weir; $H_o = h_w + (V_a)^2/2g$; V_a : velocity of approach; $V_a = Q / (BH)$; Q: total incoming discharge; B: width of the approaching channel; H: depth of flow in the approaching channel; b_w : width of weir; h_w : head of water over the weir; Q_c : discharge through the culvert; A_o : cross sectional area of the culvert; R_o : hydraulic radius of the culvert; C_D : discharge coefficient of the culvert was taken as (0.75); n: Manning roughness coefficient of the culvert material; L: length of the culvert; h_t : tailwater depth downstream the culvert.

CHAPTER 3

THEORETICAL ANALYSIS

3.1 General

Several theoretical calculations of discharge measurement for weirs and culverts were developed since the 19th century. The theoretical part of this work presents an analysis of the free flow through and over the combined structure, the upper part of the structure acts as a broad crested weir, while the lower part acts as a culvert. Dimensional analysis was performed to obtain the dimensionless parameters that affect on the coefficient of discharge. To obtain the theoretical discharge through the combined structure, equations of flow over broad crested weir and flow through culverts were used.

3.2 Flow Thought the Culvert

The hydraulic performance of culvert flow is based on the characteristics of the barrel flow (free surface flow, orifice flow or pipe flow) conditions which depend on its length, roughness, gradient and upstream and downstream water levels [24].

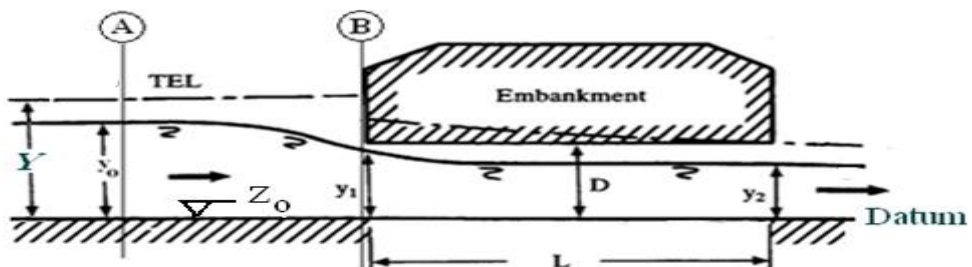


Figure 3.1 Culvert flow (R. E. Featherstone & C. Nalluri) .

Based on the factors mentioned above and with reference to (Fig. 3.1), the flow through the culverts can be classified into seven types as shown in table (3.1) below.

Table 3.1 Types of flow through Culvert (R. E. Featherstone & C. Nalluri).

N o.	y_o / D	y_o, y_c, y_2, D	Culvert length (L)	Longitudinal slope (S_o)	Culvert behaviour	Flow type
Free entrance conditions						
1	$y_o / D < 1.2$	$y_o > y_c < y_2 < D$	any length	mild slope	open channel	subcritical
2	$y_o / D < 1.2$	$y_o > y_c > y_2 < D$	any length	mild slope	open channel	subcritical
3	$y_o / D < 1.2$	$y_o < y_c > y_2 < D$	any length	steep slope	open channel	supercritical
4	$y_o / D < 1.2$	$y_o < y_c < y_2 < D$	any length	steep slope	open channel	supercritical
Submerged entrance conditions						
5	$y_o / D > 1.2$	$y_2 < D$	short	any slope	orifice flow
6	$y_o / D > 1.2$	$y_2 < D$	long	any slope	pipe flow
7	$y_o / D > 1.2$	$y_2 > D$	any length	any slope	pipe flow

Applying the energy equation to the free surface flow of Figure 3.1 between sections (A) & (B), obtaining:

$$z_o + \alpha_o \left(\frac{v_o^2}{2g} \right) + \frac{p_o}{\gamma} = z_1 + \alpha_1 \left(\frac{v_1^2}{2g} \right) + \frac{p_1}{\gamma} + h_f \quad (3.1)$$

The velocity varies across the section, the mean of the velocity head $(v^2/2g)_{\text{mean}}$ is not equal to $(v^2/2g)$, where the subscript mean refers to the mean value over the

cross section. The ratio of these quantities is called the Coriolis coefficient [25], denoted, α , which is equal or larger than (1) but rarely exceeds (1.15). For a uniform velocity distribution $\alpha=1$.

If the energy Equation (3.1) is rewritten in term of the mean velocity head, the later must be transformed as:

$$z_0 + \frac{v_0^2}{2g} + \frac{p_0}{\gamma} = z_1 + \frac{v_1^2}{2g} + \frac{p_1}{\gamma} + h_f \quad (3.2)$$

Since $p_0 = p_1 = p_{atmosphere}$, and for horizontal bed $z_0 = y_0$ & $z_1 = y_1$

$$y_0 - y_1 = \frac{v_1^2}{2g} - \frac{v_0^2}{2g} + h_f \quad (3.3)$$

The head loss (h_f) was expressed by Darcy and Weisbach as:

$$h_f = f \frac{L v^2}{D 2g} \quad (3.4)$$

The effect of frictional head loss (h_f) was neglected, since the bed plate of the flume is smooth and the distance (L) between sections (A) & (B) is short, Eq. (3.2) will reduce to:

$$v_1 = \sqrt{2g \left(y_0 - y_1 + \frac{v_0^2}{2g} \right)} \quad (3.5)$$

From the continuity:

$$Q = Av \quad (3.6)$$

Substituting Eq. (3.5) in Eq. (3.6), and for $\left(y_0 + \frac{v_0^2}{2g} \right)$ by (Y) results:

$$Q_c = \frac{\pi}{4} D^2 \sqrt{2g(Y - y_1)} \quad (3.7)$$

Experimental results showed that the actual discharge Q_{act} is smaller than the theoretical discharge Q_{theo} that obtained from Eq. (3.7) for the following two reasons:

1. The size of the jet that left the culvert entrance is smaller than the actual size of the culvert.
2. The viscous shear effect between the edge of the orifice and the water.

When the effect of the two reasons taken into account a discharge coefficient (C_d), is introduced to Eq. (3.7).

French (1986)[7], gave the discharge equation for culvert flow when it acts as an orifice which is the same as the derived equation (3.7), and he takes the upstream total head from the bottom of the culvert (i.e. he cancelled the (y_1) term) as given below:

$$(Q_c)_{act} = C_d \frac{\pi}{4} D^2 \sqrt{2g(Y)} \quad (3.8)$$

3.3 Flow over the BroadCrested Weir

The flow in any open channel may become critical if the channel bottom is raised by a specified amount. If the raised part of the channel is of sufficient length in the direction of flow, then the flow may be critical and the streamlines may be parallel to the weir. This may be utilized for flow measurement [4].

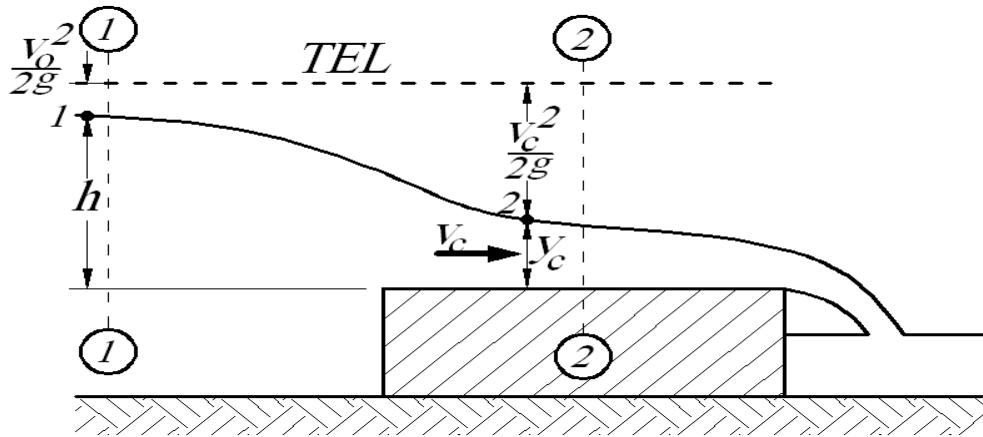


Figure 3.2 Flow over broad crested weir (M. Hanif Chaudhry).

If it is assumed that the flow on the weir in Figure (3.2) is critical, and the weir crest is horizontal, applying the energy equation to the free surface flow between points 1 & 2, obtaining:

$$h + \alpha_0 \frac{v_0^2}{2g} + \frac{p_1}{\gamma} = y_c + \alpha_c \frac{v_c^2}{2g} + \frac{p_2}{\gamma} + h_f \quad (3.9)$$

Assuming that head losses (h_f) between sections (1) and (2) are negligible, velocity distributions are uniform ($\alpha_0 = \alpha_c = 1$), and all streamlines are straight and parallel to each other, then the energy Eq. (3.9) will reduce to:

$$h + \frac{v_0^2}{2g} + \frac{p_1}{\gamma} = y_c + \frac{v_c^2}{2g} + \frac{p_2}{\gamma} \quad (3.10)$$

Since $p_1 = p_2 = p_{\text{atmosphere}}$ & $H = \left(h + \frac{v_0^2}{2g} \right)$, then Eq. (3.10) gives:

$$v_c = \sqrt{2g(H - y_c)} \quad (3.11)$$

For trapezoidal weir section:

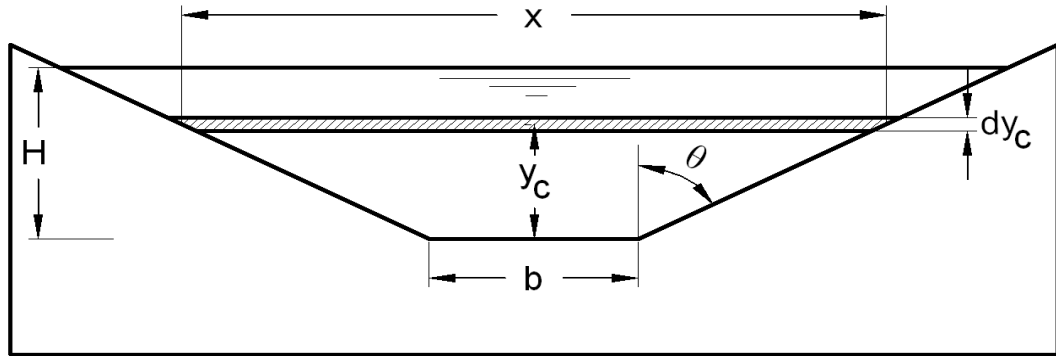


Figure 3.3 broad crested weir with trapezoidal cross section

By taking a horizontal strip in the flow section at height y_c of length x and width dy_c :

$$x = b + 2 y_c \tan \theta \quad (3.12)$$

Area of this strip is then determined by:

$$dA = x dy_c \quad (3.13)$$

From Eq. (3.11) the critical velocity through this strip element is given by

$v_c = \sqrt{2g(H - y_c)}$ and the discharge (dQ) is:

$$dQ = v_c dA_c = \sqrt{2g(H - y_c)} (b + 2 y_c \tan \theta) dy_c \quad (3.14)$$

Integrating (dy_c) through the section of flow, gives:

$$Q_w = \int_0^H \sqrt{2g(H - y_c)} (b + 2 y_c \tan \theta) dy_c \quad (3.15)$$

Evaluating of the integration yields:

$$Q_w = \sqrt{2g} \left[-\frac{2}{3} (b + 2 y_c \tan \theta) (H - y_c)^{\frac{3}{2}} - \frac{8}{15} \tan \theta (H - y_c)^{\frac{5}{2}} \right]_0^H \quad (3.16)$$

Substituting limits of the integration gives:

$$Q_w = \left(\frac{2}{3} \sqrt{2g} b H^{3/2} + \frac{8}{15} \sqrt{2g} H^{5/2} \tan \theta \right) \quad (3.17)$$

Since Eq. (3.17) had derived based on the assumption that all streamlines of water flowing on the weir crest are horizontal, and the effect of viscosity and surface tension were neglected. Hence the discharge obtained from Eq. (3.17) is greater than the actual discharge; therefore a discharge coefficient is to be added to this equation, resulting:

$$(Q_w)_{act} = C_d \left(\frac{2}{3} \sqrt{2g} b H^{3/2} + \frac{8}{15} \sqrt{2g} H^{5/2} \tan \theta \right) \quad (3.18)$$

Subramany, K. (1986) [9], gave the discharge equation for weirs of trapezoidal cross sections which is the same as the derived equation (3.18)

3.4 Combined Structure Flow

The flow through the combined structure Fig (3.4) may be free when both the flow over weir and the flow through the culvert are free and it is termed submerged when the flow through the culvert is submerged (and the flow over the weir may or may not be submerged).

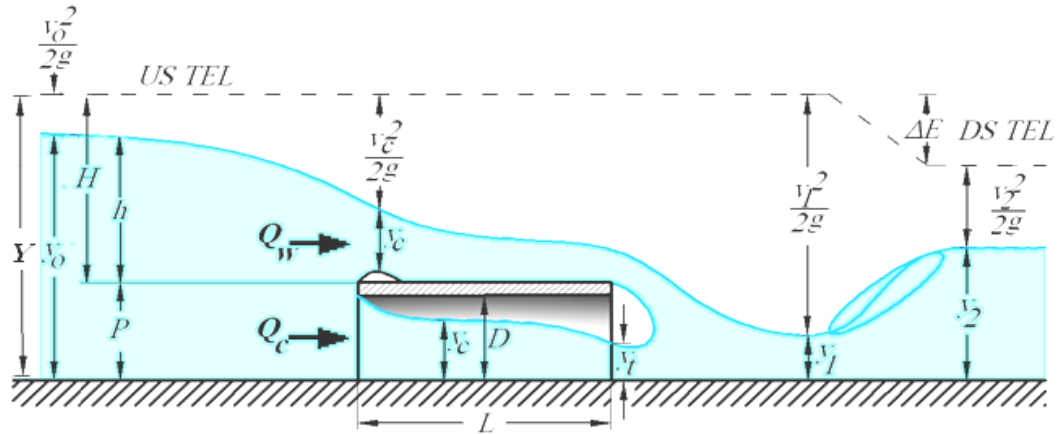


Figure 3.4 combined structure flow(M. HanifChaudhry)

The simultaneous discharge can be obtained by summing the overflow discharge over the broad crested weir and the underflow discharge that passed through the culvert.

$$Q_t = Q_w + Q_c \quad (3.19)$$

Substituting for Q_w and Q_c by Eqns. (3.17) and (3.7):

$$(Q_t)_{act} = C_d \left[\left(\sqrt{2g} \frac{2}{3} b H^{3/2} + \sqrt{2g} \frac{8}{15} H^{5/2} \tan \theta \right) + \frac{\pi}{4} D^2 \sqrt{2gY} \right] \quad (3.20)$$

Where(C_d) is a discharge coefficient to account for the combination between the flow over the weir and that through the culvert. The combined discharge coefficient (C_d) is to be determined experimentally.

3.5 Dimensional Analysis

Dimensional analysis and π -theorem are powerful tools for solving many theoretical and experimental physical studies. The basis of dimensional analysis is to condense the number of separate variables involved in a particular type of physical system into a smaller number of non-dimensional groups of the variable. The arrangement of the

variables in the groups is generally chosen so that each group has a physical significance. All physical parameters can be expressed in terms of a number of basic dimensions, in engineering the basic dimensions, Mass (M), Length (L) and Time (T) are sufficient for this purpose [24]. The Buckingham (Pi Theorem) was used to develop dimensionless parameters, the Pi (π) terms, from the variables. Five parameters are used to describe the geometry of the broad crested weir and the culvert as shown in Fig (3.5)

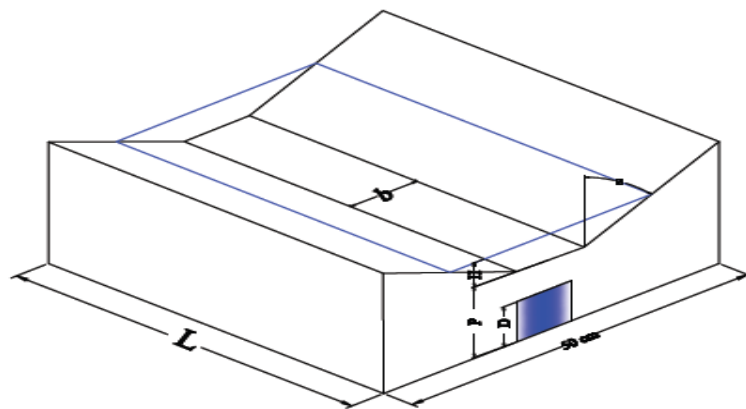


Figure 3.5 Definition of symbolism for the combined structure

The discharge over broad crested weir and through the culverts depends on:

- 1- Geometry of the structure, which is described by:
 - a- Bottom width of the weir (b) .
 - b- Weir height (P).
 - c- Weir side slopes ($\tan \theta$).
 - d- Upstream total head above the weir crest (H).
 - e- Weir length (L).
 - f- Diameter of the culvert (D).
- 2- Fluid (water properties) which they are:
 - a- Weight density (γ).

b- Surface tension (σ).

c- Viscosity (μ).

d- Mass density (ρ).

3-Fluid characteristics which is: the gravitational acceleration (g).

The discharge passed through the combined structure depends on the variables mentioned above, and can be expressed as the following relation:

$$Q = \phi[g, H, P, b, L, \tan\theta, D, \rho, \mu, \sigma] \quad (3.21)$$

Taking variables (H) from the geometry of the structure, (ρ) from fluid water properties and (g) from fluid characteristics as repeating variables, the (π) terms can be expressed as:

$$\pi_1 = \rho, g, H, Q; \quad \pi_2 = \rho, g, H, P; \quad \pi_3 = \rho, g, H, b; \quad \pi_4 = \rho, g, H, L; \pi_5 = \rho, g, H, D; \quad \pi_6 = \rho, g, H, \tan\theta; \quad \pi_7 = \rho, g, H, \mu; \pi_8 = \rho, g, H, \sigma$$

For π_1 :

$$\pi_1 = M^0 L^0 T^0 = (ML^{-3})^\alpha (LT^{-2})^\beta (L)^\gamma (L^3 T^{-1})^{+1}$$

$$\text{For M: } \alpha = 0; \text{ For T: } 0 = -2\beta - 1; \beta = \frac{-1}{2}; \text{ For L: } 0 = -3\alpha + \beta + \gamma + 3; \gamma = \frac{-5}{2}$$

$$\pi_1 = \frac{Q}{\sqrt{g}H^{5/2}}$$

$$\text{For } \pi_2; \pi_2 = M^0 L^0 T^0 = (ML^{-3})^\alpha (LT^{-2})^\beta (L)^\gamma (L)$$

$$\text{For M: } \alpha = 0; \text{ For T: } 0 = -2\beta; \beta = 0; \text{ For L: } 0 = -3\alpha + \beta + \gamma + 1; \gamma = -1;$$

$$\pi_2 = \frac{P}{H}$$

$$\text{By the same manner: } \pi_3 = \frac{b}{H}, \pi_4 = \frac{L}{H} \text{ and } \pi_5 = \frac{D}{H}$$

$$\text{For } \pi_6: \pi_6 = \rho^\alpha g^\beta H^\gamma \tan\theta$$

Since $(\tan\theta)$ is a dimensionless variable; $\pi_6 = \tan\theta$

$$\text{For } \pi_7: \pi_7 = M^0 L^0 T^0 = (ML^{-3})^\alpha (LT^{-2})^\beta (L)^\gamma (ML^{-1}T^{-1})$$

$$\text{For M: } 0 = \alpha + 1, \alpha = -1; \text{For T: } 0 = -2\beta - 1; \beta = \frac{-1}{2};$$

$$\text{For L: } 0 = -3\alpha + \beta + \gamma - 1; \gamma = \frac{-3}{2}; \pi_7 = \frac{\mu}{\rho\sqrt{gH^{3/2}}} = \frac{\mu}{\rho\sqrt{gHH}}$$

$$\text{Substituting for } V = \sqrt{gH}; \pi_7 = \frac{\mu}{\rho VH} = \frac{1}{\text{Re}}$$

$$\text{For } \pi_8: \pi_8 = M^0 L^0 T^0 = (ML^{-3})^\alpha (LT^{-2})^\beta (L)^\gamma (MT^{-2})$$

$$\text{For M: } 0 = \alpha + 1; \alpha = -1; \text{For T: } 0 = -2\beta - 2; \beta = -1;$$

$$\text{For L: } 0 = -3\alpha + \beta + \gamma; \gamma = -2; \pi_8 = \frac{\sigma}{\rho g H^2} = \frac{\sigma}{\rho V^2 H} = \left(\frac{1}{\text{We}}\right)^2$$

The functional relationship then becomes:

$$\pi_1 = \Phi[\pi_2, \pi_3, \pi_4, \pi_5, \pi_6, \pi_7, \pi_8] \quad (3.22)$$

Substituting the (π) terms obtained into Eq. (3.22):

$$\frac{Q}{\sqrt{gH^{5/2}}} = \Phi\left[\frac{H}{P}, \frac{H}{b}, \frac{H}{L}, \frac{H}{D}, \tan\theta, \text{Re}, \text{We}\right] \quad (3.23)$$

Dimensionless parameters $(\pi_7 \& \pi_8)$ shows that both Reynolds number (Re) and Weber number (We) are varies proportionally with (V), and (V) varies proportionally with (H) and (Re & We) varies inversely with $(\mu \& \sigma)$ respectively, therefore the effect of viscosity and surface tension decrease with increase in (H) and it can be neglected if the head (H) is not too small (not less than 6mm) [27], for these reasons

and using same fluid in which (ρ , σ & μ) are constant , terms (Re) and (We) can be terminated from Eq. (3.23) to form the new relation:

$$\frac{Q}{\sqrt{g}H^{5/2}} = \phi \left[\frac{H}{P}, \frac{H}{b}, \frac{H}{L}, \frac{H}{D}, \tan\theta \right] \quad (3.24)$$

Since (C_d) is a dimensionless parameter and similar in form to the dimensionless term (π_1), it can be substituted for (π_1) in the evaluation of the problem. This allows the evaluation of the coefficient of discharge as a function of the geometrical parameters:

$$C_d = \phi \left[\frac{H}{P}, \frac{H}{b}, \frac{H}{L}, \frac{H}{D}, \tan\theta \right] \quad (3.25)$$

Equation (3.25) is for the Discharge coefficient through the combined structure, and for the Broad Crested Weir, terms concerned to the culvert flow to be removed, then it will be reduced to:

$$C_d = \phi \left[\frac{H}{P}, \frac{H}{b}, \frac{H}{L}, \tan\theta \right] \quad (3.26)$$

And for the flow through the culvert pipe, terms concerned to the Broad Crested Weir flow to be removed and the equation will be:

$$C_d = \phi \left[\frac{Y}{L}, \frac{Y}{D} \right] \quad (3.27)$$

The actual form of these functions must be determined by statistical analysis of the experimental data.

CHAPTER 4

EXPERIMENTAL SETUP AND METHODOLOGY

4.1 General

Experiment works were performed in the laboratory flume of the Hydraulic Laboratory of Engineering College, Sallahadin University. Laboratory apparatus to simulate flow over Broad crested weir and through culverts has been used to collect discharge and water depth measurements.

The methodology of the study is designed to achieve the objectives of the study based on the prescribed on the scope of work. The measurements presented in this study are intended to provide useful information regarding the variety of flow conditions (including overtopping, through the culvert and over the weir).

4.2 Experimental Setup

The apparatus and instruments used in this study are mentioned in this chapter as described below each in detail.

4.2.1 The Flume

The experiments were conducted on a smooth toughened glass sided and smooth painted bed steel plate flume of 12 m working length. The flume cross sectional area is 50 cm wide and 50 cm deep. The longitudinal slope of the Flume can be adjusted mechanically by two hydraulic jacks raised and lowered manually to establish the required slope. At the downstream end, the flume was equipped with a vertically

moving tail gate to control the tailwater depth. A pair of steel pipe rails was fixed on the top of the side walls throughout the working length to support the point gages. The upstream end of the flume was connected to the stilling basin of internal dimensions (2.5 m length, 0.70 m width and 0.87 m depth) by a smooth thin steel plate, provided at its end with a series of alternate mesh screens to dissipate the energy of the incoming flow from the overhead tank. Water supplied to the flume from an underground concrete storage tank of internal dimensions (7.5 m length, 2.5 m width and 1.0 m depth). Water drawn from the underground storage tank by an electrically driven centrifugal pump through a 6 inch diameter Steel pipe to the overhead tank providing a total discharge of (50 lit/sec). Fig (4.1) and Fig (4.2) shows the Flume.



Figure 4.1 The Flume use din the study

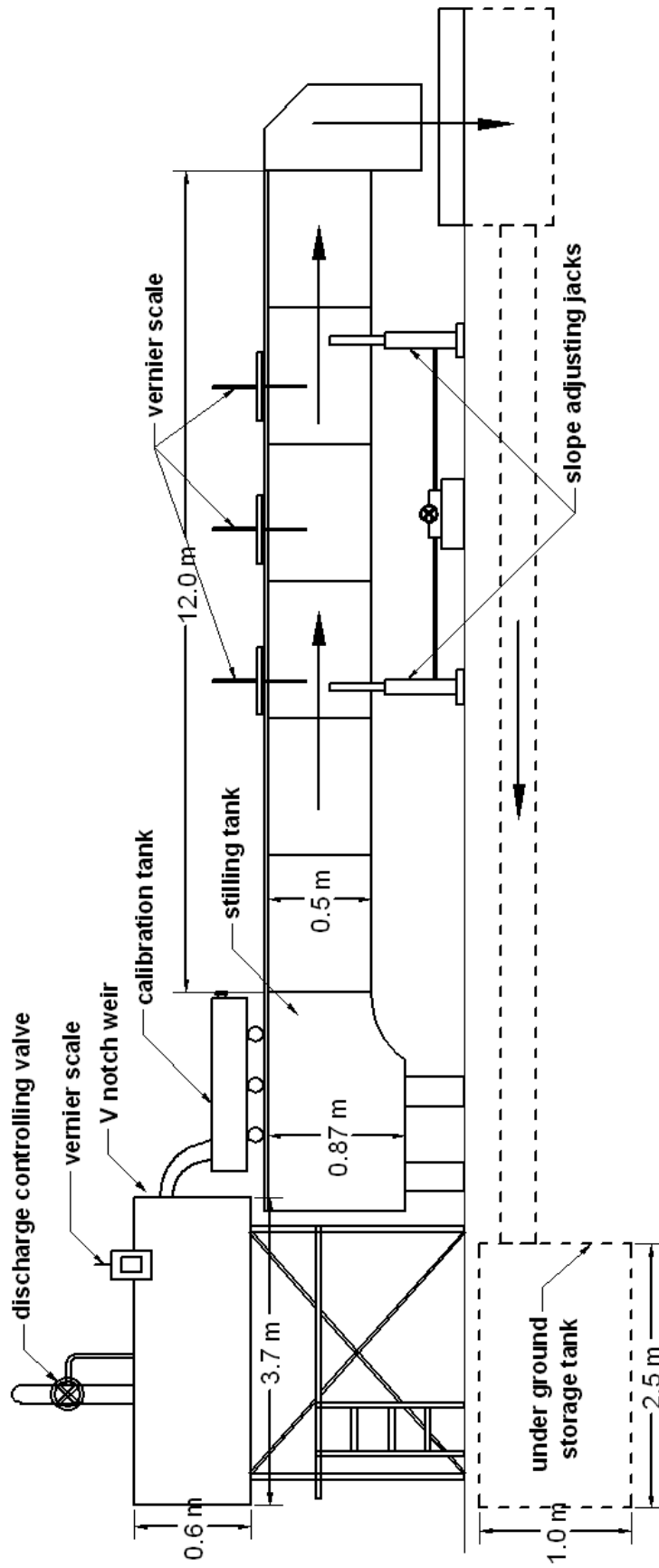


Figure 4.2 The Flume used in the study

4.2.2 The Overhead Tank

A box shape tank of internal dimensions 3.7 m length, 0.8m width and 0.6 m depth, made from thick steel plate fixed on a steel frame elevated to the required height. Water that pumped into the over head tank passes through a series of alternate mesh screens to dissipate its turbulence and energy before reaching the upstream of the V-notch weir and overflowing to the flume, discharge controlled by two control valves one of 6" dia. and the other of 1.5" dia.



Figure 4.3 The Overhead tank and the V-notch weir used in the study

4.2.3 The V-notch weir

The discharge in the Flume was measured by means of a V-notch weir Fig (4.4) located at the end of the overhead tank. The head of water above the V-notch was measured by a point gage with a vernier scale of 0.05mm accuracy located 80 cm

upstream of the V-notch weir placed in a small box tank fixed to the right side of the over head tank and connected from bottom to the over head tank so that the depth of water in the side tank is the same in the overhead tank and the water surface is in static condition.

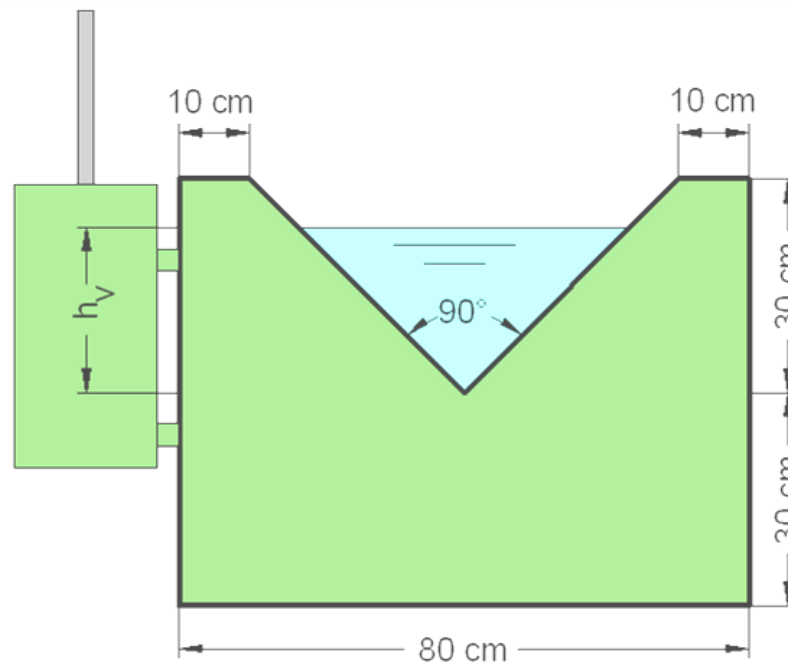


Figure 4.4 Details of the V- notch weir

4.2.4 The Measuring Tank

A box shape tank figure (4.5) manufactured for calibrating the head-discharge relation of the V-notch weir, the calibration tank manufactured with internal dimensions (1.5 m length, 1 m width and 0.3 m height) to store about 300 liters, the tank provided with six rollers (three in each side) to facilitate its movement.

The tank placed downstream of the V-notch weir and fast pulled when filled by water, the time was recorded by a stop watch of 0.01 sec accuracy. In each run the volume of water, time and the head above the V-notch was recorded.



Figure 4.5 The measuring tank manufactured for the calibration of the V-notch weir

For several water depths above the V-notch weir between (5 to about 28 cm), the measuring tank placed under the weir and for a reasonable volume of water the time was recorded, this procedure was repeated two times for each depth of water above the weir and the data Table (4.1), plotted to the curve shown in Fig (4.6), and the following relation was obtained which has a determination coefficient (R²) of 0.999.

$$Q = 0.0195h_v^{2.398}$$

Where: Q: discharge in l/sec, and; h_v: head of water above the V-notch weir in cm.

Table 4.1 Calibration Data of the V-notch weir.

$h_v(cm)$	Trial one			Trial two			Average Ql/sec
	time (sec)	volume (l)	Q_1 (l/sec)	time (sec)	volume (l)	Q_2 (l/sec)	
0			0			0	0
5.155	221.19	218.025	0.98569	237.79	236.1	0.99289	0.98929
9.365	55.27	229.725	4.15641	64.94	268.275	4.13112	4.14377
12.115	32.58	251.925	7.7325	31.35	242.4	7.73206	7.73228
14.915	17.37	229.35	13.2038	18.48	234.3	12.67857	12.94119
16.5	16.88	272.7	16.15521	17.91	287.625	16.05946	16.10734
18.31	14.11	297.225	21.06485	13.07	282.6	21.62204	21.34344
19.455	11.02	264.75	24.0245	10.49	239.7	22.85033	23.43742
21.5	7.79	246.6	31.65597	7.57	245.325	32.40753	32.03175
24.225	5.95	241.875	40.65126	7.34	278.625	37.95981	39.30553
24.565	5.6	222.675	39.76339	4.14	175.2	42.31884	41.04112
25.975	5.21	240	46.06526	6.29	316.65	50.34181	48.20354

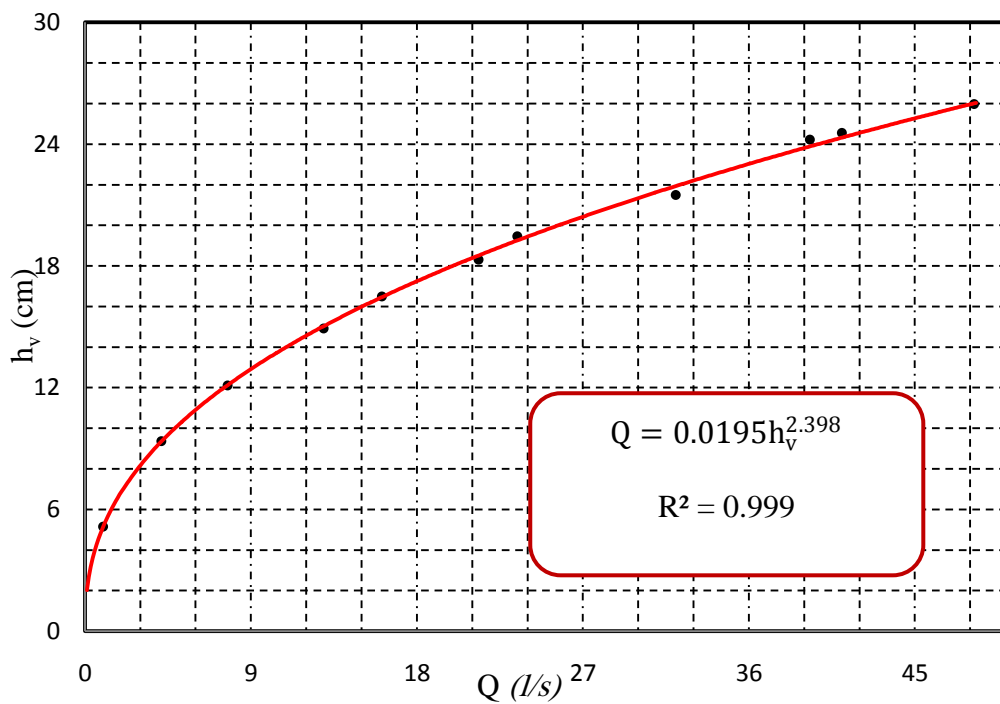


Figure 4.6 Calibration curve of the V- notch weir

4.2.5 Point Gages for Depth Measurement

The water depth in the test flume was measured by means of three precision point gauges figure (4.7). The vernier scale of the point gages permitted depth readings with an accuracy of 0.5 mm. The point gages were mounted on a carriage which moved on a pair of rails fixed on the top of the side walls of the test flume. This traversing arrangement enable three degree freedom of movement and enabled the gage reading at any arbitrary point in the area of interest to be taken by moving the carriage and the point gage.



Figure 4.7 Point gages with its carriage

4.3 Construction of the Models

The selection of models material and dimensions are based on the facilities of the laboratory and to produce minimum roughness of the models. Models constructed from glass and fixed by silicon.



Figure 4.8 One of the models

Twelve (12) models constructed, these models divided into (4) groups of similar culvert diameter but of three different side slopes ($\tan \theta$), the height (P) determined by adding the pipe thickness (T) to the pipe diameter multiplied by 1.2, to obtain full submergence at the culvert inlet.

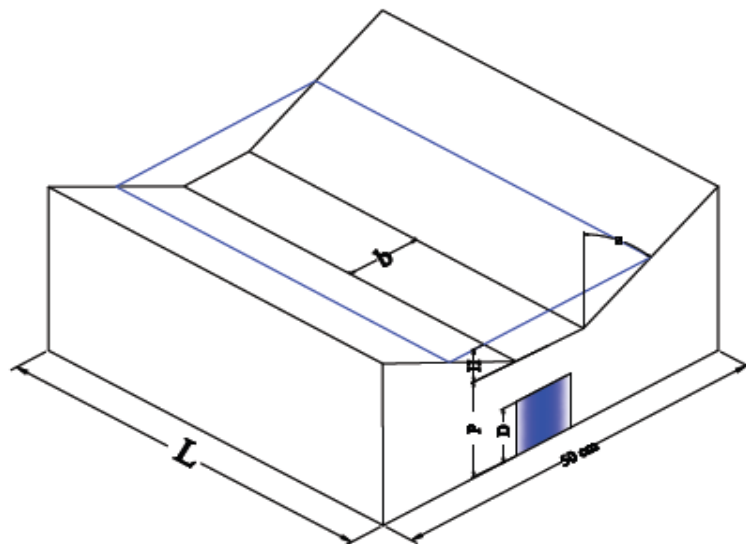


Figure 4.9 Definition of symbolism of the models

4.4 Testing Program

Before starting the tests, the flume was levelled by use of a level instrument, so that the longitudinal bed slop was set to zero. Models placed at a distance of (9 m) from the upstream end, the models assembled in the canal and fixed with the flume sides by a special paste to prevent seepage of water.

For each model, the testing program was divided into three phases:

1. Only flow through the culvert, this was achieved by fixing a play wood block on the upstream corner of the model to prevent flow over the weir.
2. Only flow over the weir, this was achieved by closing inlet of the culvert.
3. Flow over the weir and through the culvert.

In each state of flow the discharge is gradually increased such that the behaviour of the flow is clearly recognized, each flow state consists of a number of runs. For each run, the depth of water above the V-notch weir (h_v) and the corresponding uniform water depth in the canal upstream of the tested model (y_o) were measured.

CHAPTER 5

DATA ANALYSIS AND DISCUSSION OF RESULTS

5.1 General

The main objective of data analysis is to develop an equation for discharge coefficient (C_d) as a function of parameters obtained from dimensional analysis performed in chapter three for each of the three flow states (culvert, weir and combined flow), for this purpose several forms of equations were used, then the best one was used by using SPSS program.

5.2 Head - Discharge Relations

Open channel flow measurements are typically based on measurements of flow depth, which are then correlated with discharge in head-discharge curves. Measurement of flow in open channels is essential for better management of limited supplies of water. Accurate measurement practices help to provide equitable distribution of water between competing demands. Most flow measurement structures are emplaced in a channel. They are used to determine the discharge indirectly from measurements of the flow depth. In combined structures, it is expected that there is always a discontinuity in the head-discharge rating at the point that the flow begin to over flow the upper structure and the flow behaviour changes from culvert flow to the combined flow. The head-discharge relations for each model are plotted in to three curves for the three flow states (culvert, weir and combined) as shown in Fig (5.1). It may be observed from the figures that at a given head (Y),

Adding the flow through the culvert to the flow over the weir equal to the combined flow measurements.

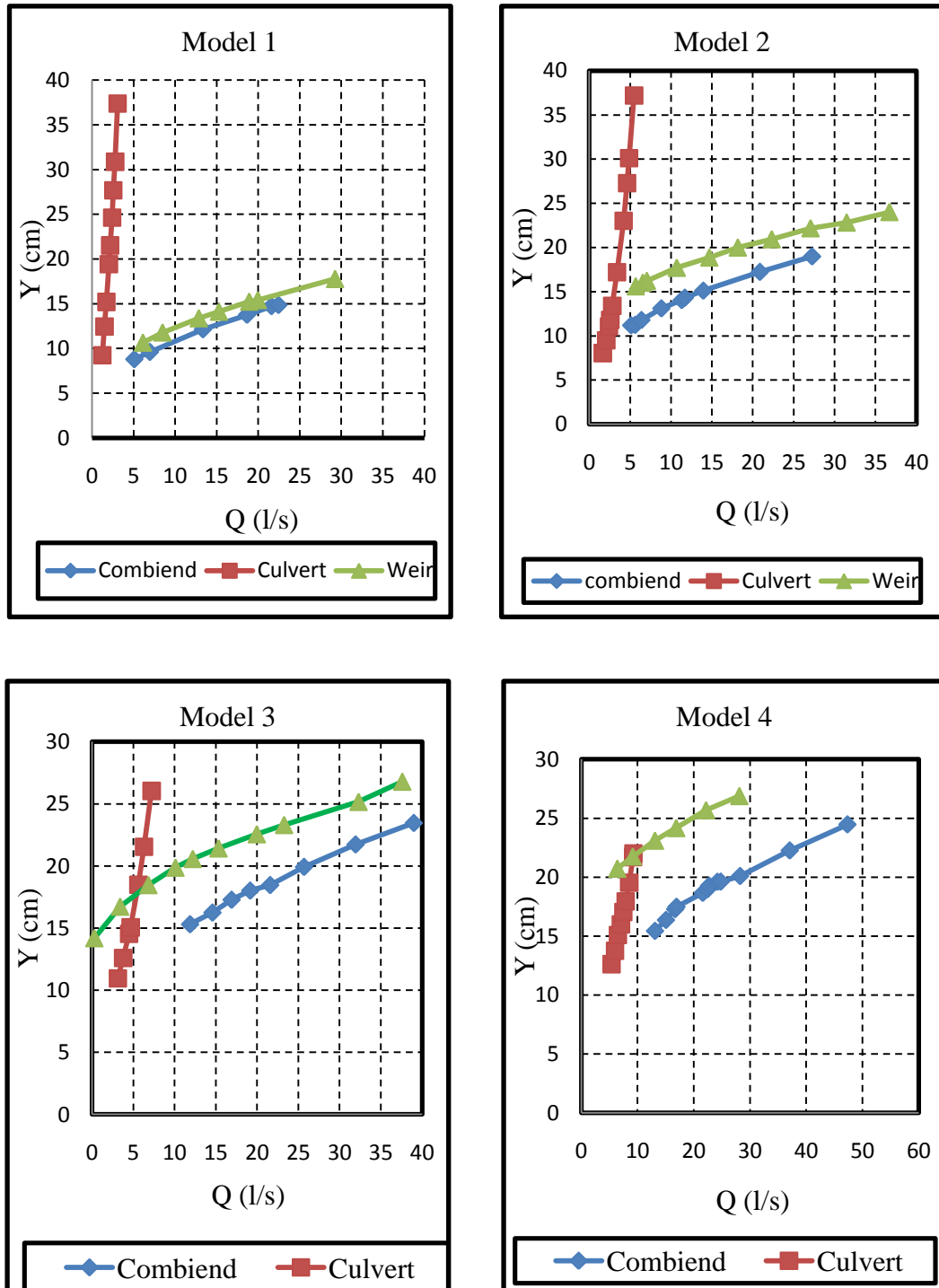


Figure 5.1 Head Discharge Relations for Models 1-4

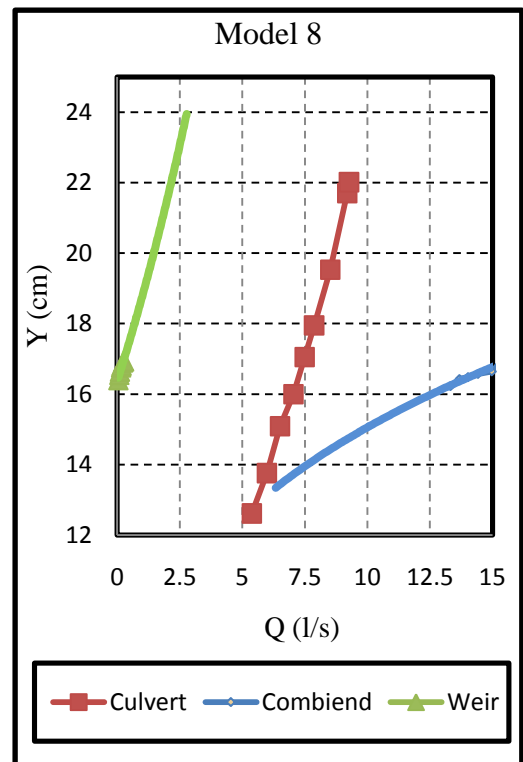
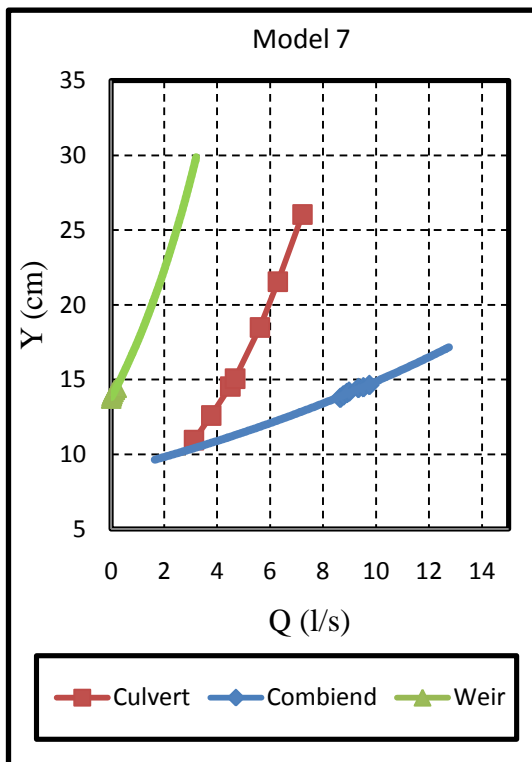
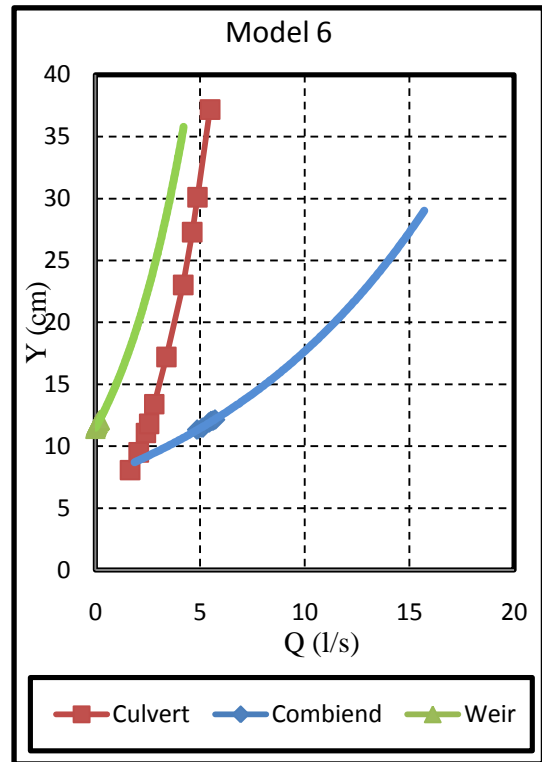
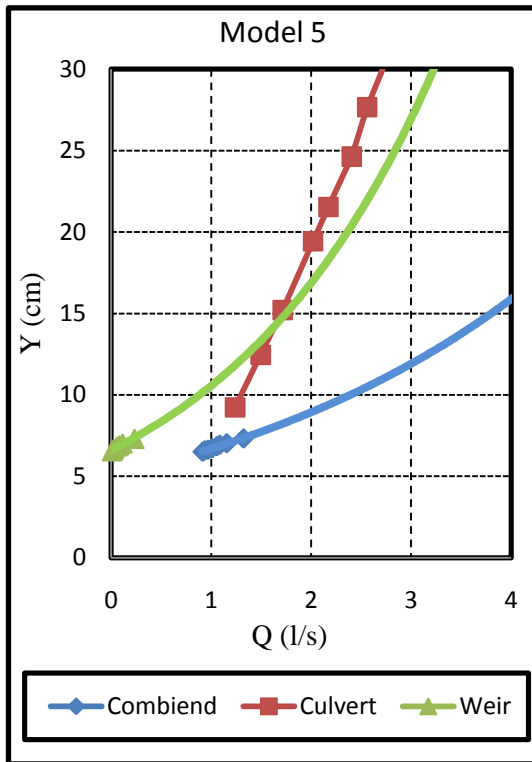


Figure 5.1 Continued, Head Discharge Relations for Models 5-8

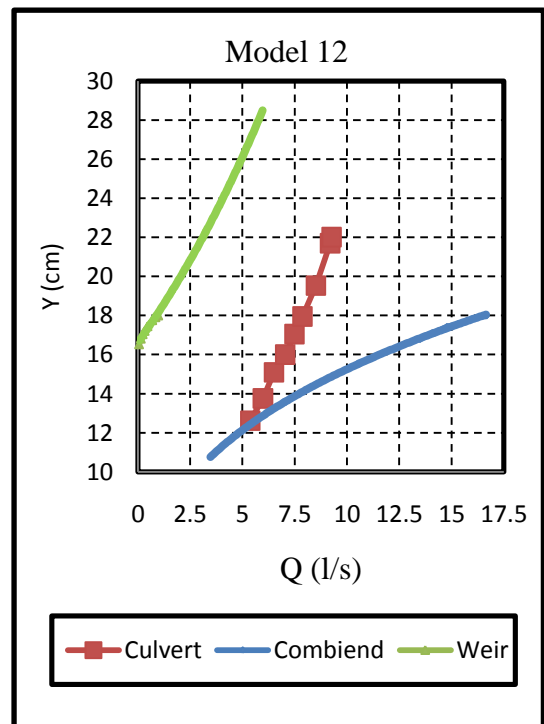
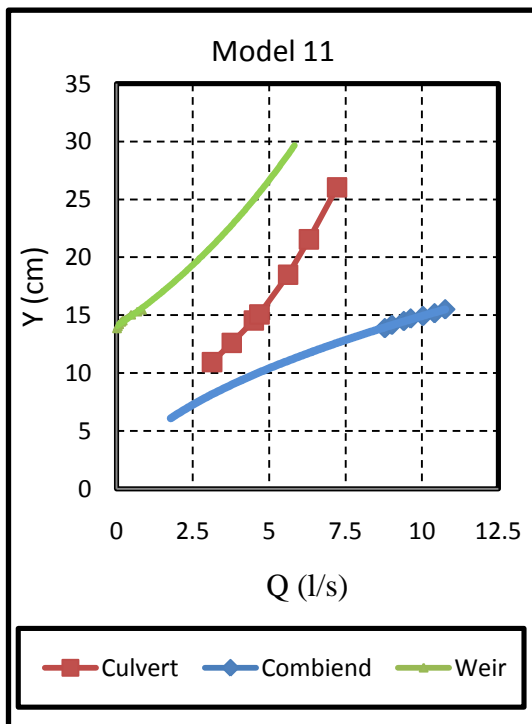
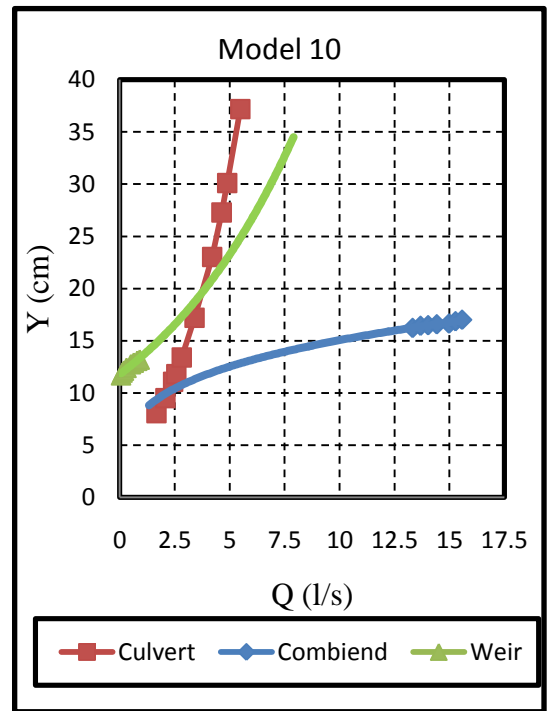
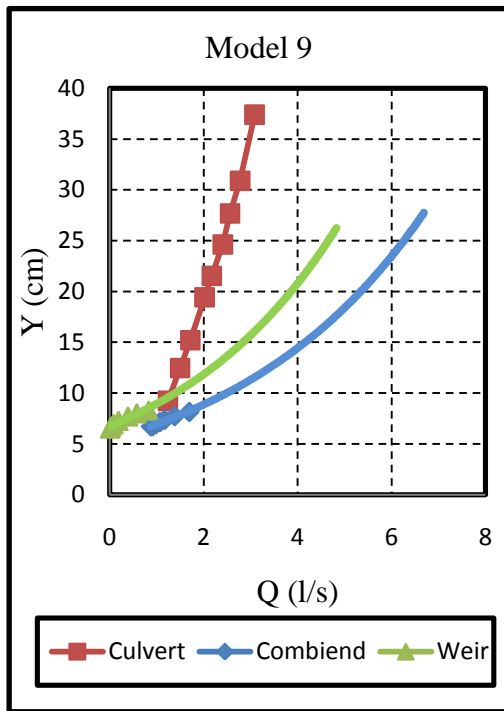


Figure 5.1 Continued, Head Discharge Relations for Models 9-12

The intersection points between culvert curves and broad crested weir curves showed in Fig (5.1) indicate that at these points both discharges are equal, below these intersection points the culvert discharge are greater than broad crested weir discharge, and above it the weir discharge is greater, and in both cases cumulating the weir and culvert discharge equals the combined structure discharge at a certain head (Y).

5.3 Effect of Weir Height (P)

It is difficult to investigate the effect of weir height (P) in the case of the combined structure flow, since it contains the culvert part and the culvert height varies with the weir height. Therefore it was studied in the case of weir flow only. The discharge values of weir models having the same lower weir crest width (b) and the same side slope angles (θ), but different in weir crest heights(P), were considered as a single data group and were plotted against the total head (H) in Fig (5.2) in order to observe the effect of (P) on the discharge coefficient. Coincides of curves of different values of (P) indicates that there is no direct significant relation between weir height (P) and (Q).

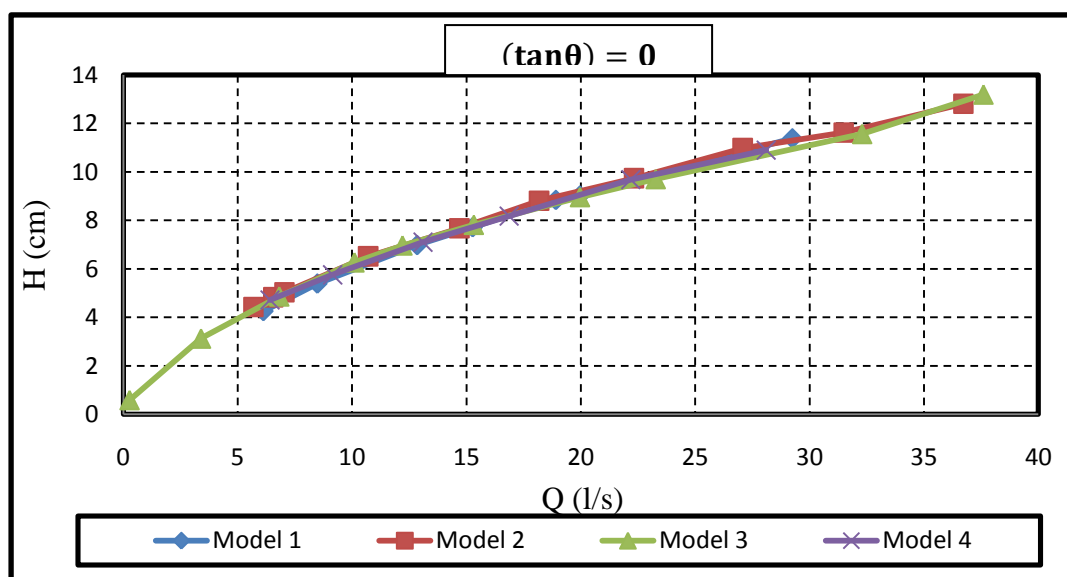


Figure 5.2 Effect of weir height (P) on the Discharge for the BCW

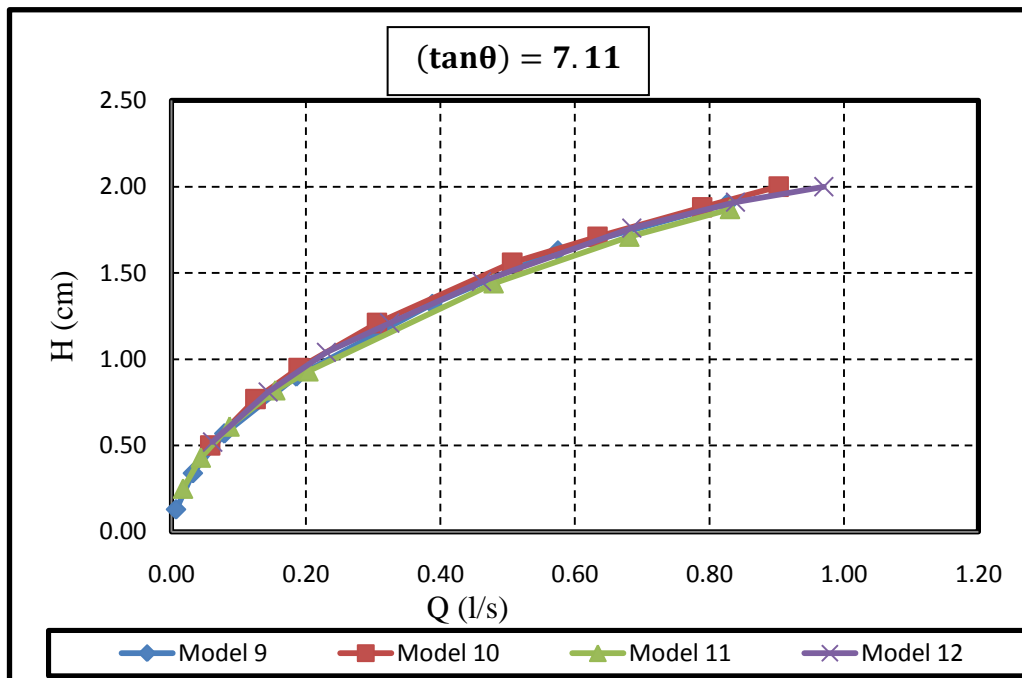
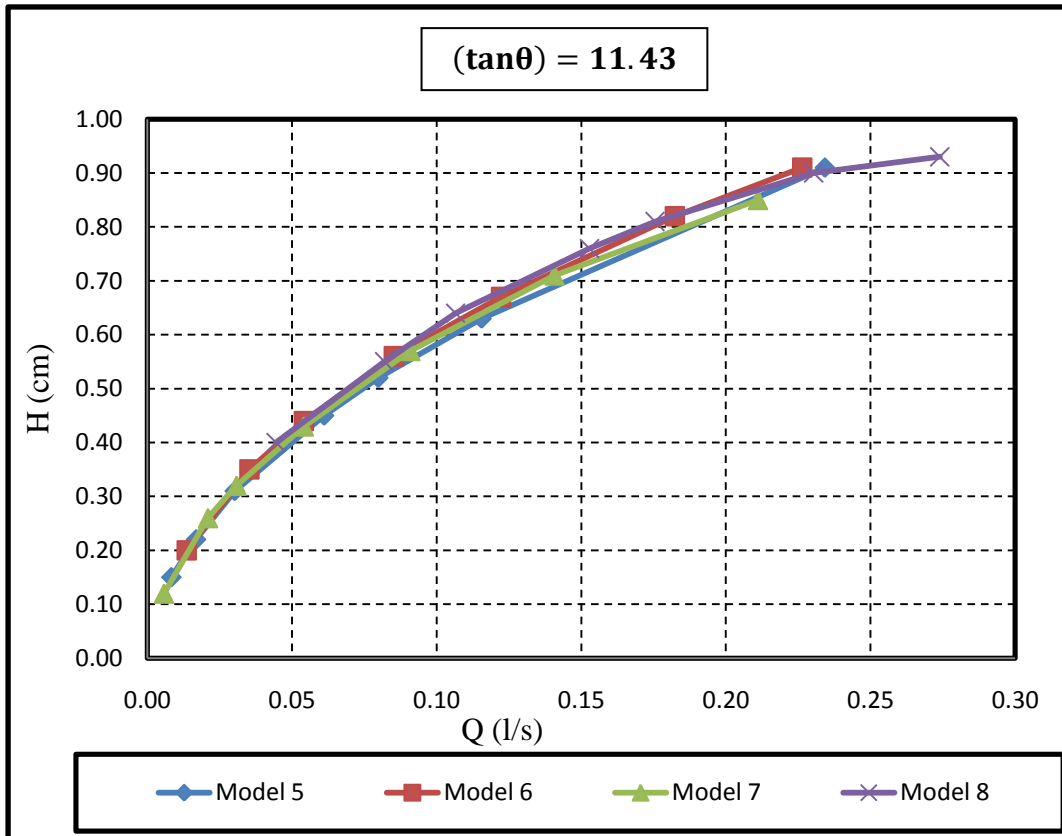


Figure 5.2 Continued, Effect of weir height (P) on the Discharge for the BCW

5.4 Effect of the Side Slope (θ)

The effect of side slope (θ) was analyzed by drawing a relation between the discharge coefficient (C_d) and the ratio of the head above the weir to the crest height (H/P) for all the present tested angles of weir side slopes (θ) as shown in Fig (5.3).

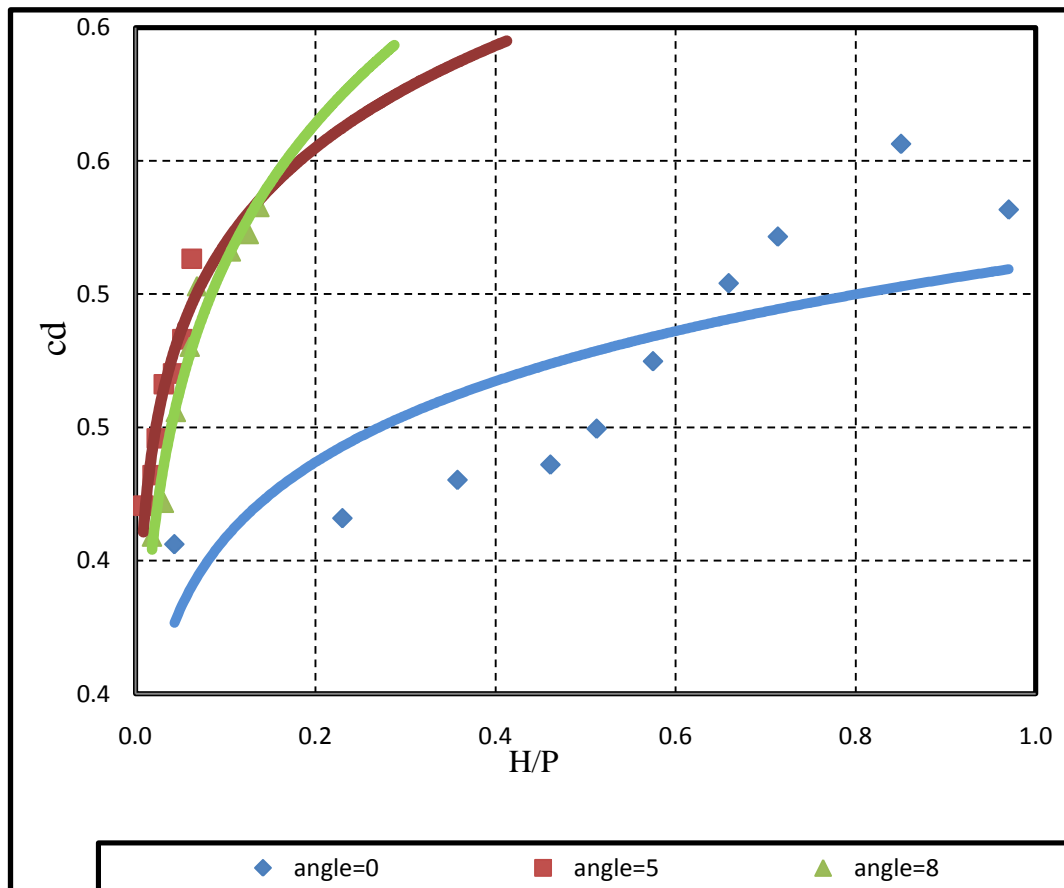


Figure 5.3 Effect of side slope on the Discharge coefficients for the various models of the combined structure

Curves of Fig (5.3) show that for a certain value of (H/P) the (C_d) value increases with decreasing in the side slope angles, this is because of decreasing the wetted parameter with decreasing in side slope angles ($\tan\theta$).

5.5 Effect of the Culvert Dimension (D)

The discharge coefficient (C_d) plotted against the ratio of upstream water depth to the culvert diameter (Y/D) together with the data obtained from the literature [Table (5.1)] for the same culvert flow condition, as shown in Fig (5.4).

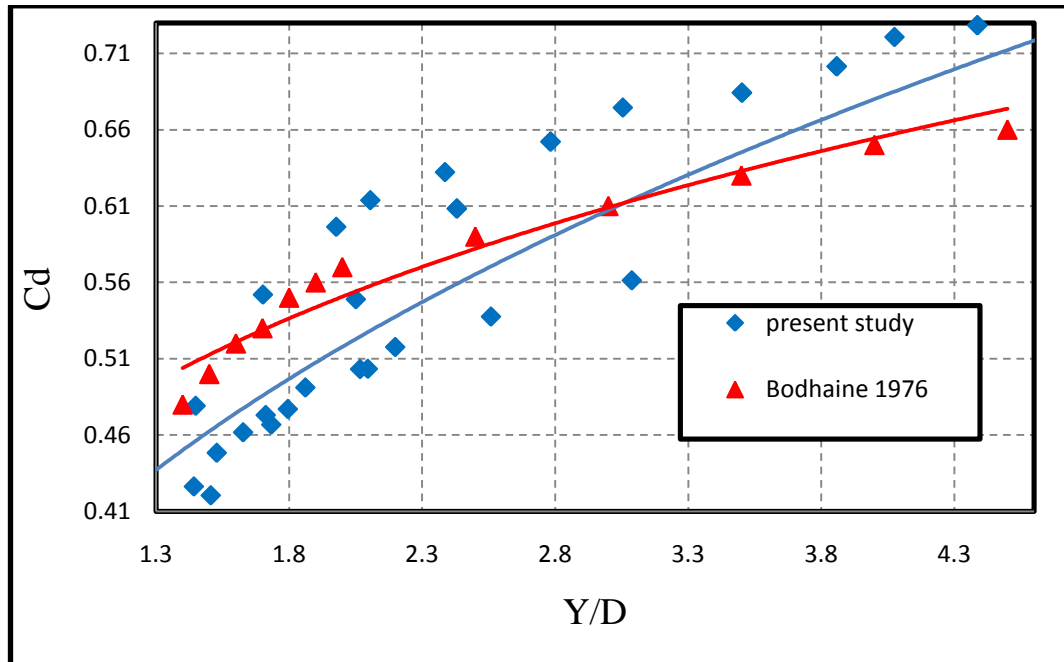


Figure 5.4 Head Discharge Coefficient Relations for culvert flow

Table 5.1 Coefficient of discharge as a function of Y/D for type 5 flow in a culvert with a flared – pipe end section (Bodhaine, 1976)

Y/D	Cd	Y/D	Cd
1.4	0.48	2.0	0.57
1.5	0.50	2.5	0.59
1.6	0.52	3.0	0.61
1.7	0.53	3.5	0.63
1.8	0.55	4.0	0.65
1.9	0.56	4.5	0.66

In order to investigate the effect of the box culvert dimension, the discharge coefficient (C_d) plotted against the upstream water depth (Y) for the box culvert

dimension used in the study as shown in Fig (5.5), which indicates that the discharge coefficient (C_d) increases with a decrease in the culvert pipe diameter for a certain upstream water depth (Y).

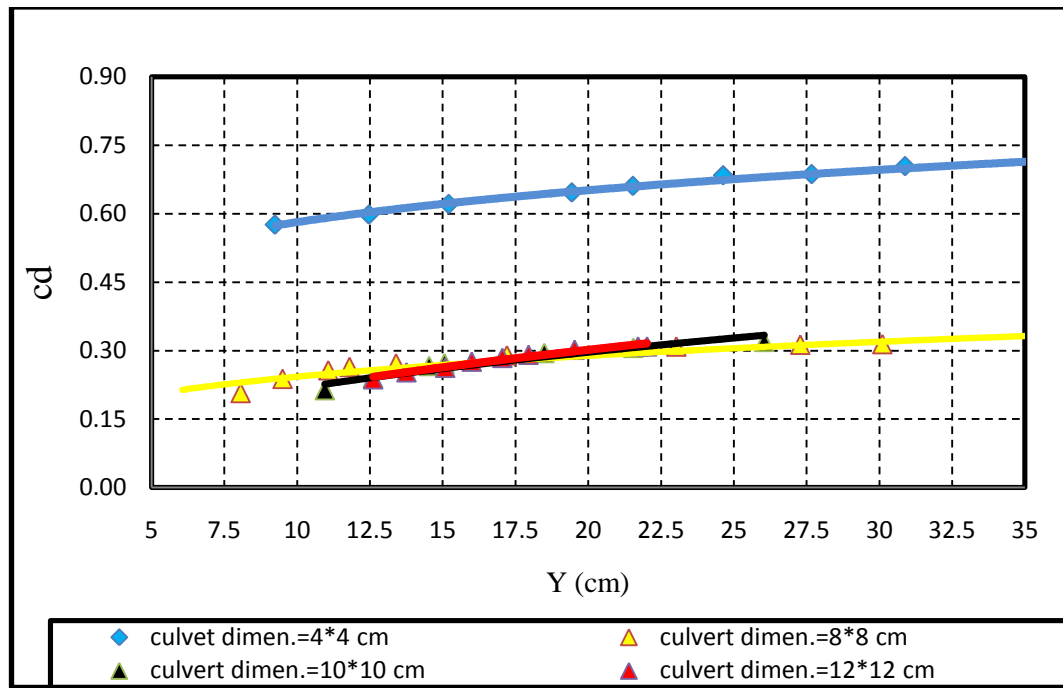


Figure 5.5 Head Discharge Coefficient Relations for culvert flow

It can be indicated from Fig (5.5) that (C_d) increases with (Y/D) for the culverts, this can be explained by the following reasons:

1. An increase in the head (Y) reduces the effect of viscosity which increase the resistance of the boundaries of the flow.
2. At low values of (Y) the effect of surface tension is clearly recognized which cause cling of the water particles to the structure body which leads to decrease the velocity of flow and the value of (C_d).
3. For constant value of (Y) the ratio of (Y/D) can be increased by reducing the value of (D) which also leads to increase the discharge coefficient (C_d) which can be seen clearly from Fig (5.6), this is because the decrease in pipe diameter decreases its parameter and then decrease in boundary resistance.

5.6 Correlations for Discharge Coefficient (Cd)

To obtain equations for the discharge coefficient (Cd), (SPSS20) statistical software was used for obtaining two types of regressions between the discharge coefficient (Cd) and dimensionless parameters obtained by dimensional analysis were tested to find the best one, they are:

1. Linear relationship between (C_d) and the rest of the parameters:

$$C_d = a + b\pi_2 + c\pi_3 + d\pi_4 + e\pi_5 + f\pi_6 \quad (5.1)$$

Where (a) to (f) are regression coefficients to be obtained from a multivariable regression of the experimental data.

2. Power function relationship between (C_d) and the rest of the parameters:

$$C_d = a(\pi_2)^b (\pi_3)^c (\pi_4)^d (\pi_5)^e (\pi_6)^f \quad (5.2)$$

Where (a) to (f) are regression coefficients to be obtained from a multivariable regression of the experimental data.

5.6.1 Discharge Coefficient Regressions for the Culvert

The linear regression yielded the following equation:

$$C_d = 0.440 - 0.384 \frac{Y}{L} + 0.098 \frac{Y}{D} \quad (5.3)$$

R Squared=0.836

The power regression yielded the following equation:

$$C_d = 0.275 \frac{\left(\frac{Y}{D}\right)^{0.51}}{\left(\frac{Y}{L}\right)^{0.239}} \quad (5.4)$$

R Squared=0.923

5.6.2 Discharge Coefficient (Cd) for the Broad Crested Weir

The multivariable linear regression yielded the following equation

$$C_d = 0.412 + 0.038 \frac{H}{P} - 0.047 \frac{H}{b} + 0.273 \frac{H}{L} - 0.001 \tan \theta \quad (5.5)$$

R Squared=0.39

The multivariable power regression yielded the following equations:

A- For $\tan(\theta) = 0$.

$$C_d = 0.553 \frac{\left(\frac{H}{P}\right)^{0.05} \left(\frac{H}{b}\right)^{2.621}}{\left(\frac{H}{L}\right)^{2.56}} \quad (5.6)$$

R Squared=0.797

B- For $\tan(\theta) > 0$.

$$C_d = 0.365 \frac{\left(\frac{H}{P}\right)^{0.07} \left(\frac{H}{b}\right)^{0.136}}{\left(\frac{H}{L}\right)^{0.065}} (\tan \theta)^{0.182} \quad (5.7)$$

$$C_d = 286.5 + 0.069 \frac{H}{P} + 0.711 \frac{H}{b} - 1.879 \frac{H}{L} - 238.5 \tan \theta - 0.02 \left(\frac{H}{P}\right)^2 - 0.6 \left(\frac{H}{b}\right)^2 + 9.269 \left(\frac{H}{L}\right)^2 + 47.71 (\tan \theta)^2 \quad (5.8)$$

R Squared=0.6

5.6.3 Discharge Coefficient (Cd) for the Combined Structure

The multivariable linear regression yielded the following equation:

$$C_d = 0.479 - 1.447 \frac{H}{P} - 0.076 \frac{H}{b} + 1.021 \frac{H}{L} + 1.044 \frac{H}{D} - 0.012 \tan \theta \quad (5.9)$$

R Squared=0.693

The multivariable power regression yielded the following equations:

A- For $\tan(\theta) = 0$

$$C_d = 0.832 \frac{\left(\frac{H}{P}\right)^{1.265} \left(\frac{H}{L}\right)^{0.771}}{\left(\frac{H}{b}\right)^{0.689} \left(\frac{H}{D}\right)^{1.277}} \quad (5.10)$$

R Squared=0.725

B- For $\tan(\theta) > 0$.

$$C_d = 0.394 \frac{\left(\frac{H}{b}\right)^{0.018} \left(\frac{H}{L}\right)^{0.092} \left(\frac{H}{D}\right)^{1.272}}{\left(\frac{H}{P}\right)^{1.292}} (\tan \theta)^{0.06} \quad (5.11)$$

R Squared=0.671

After regressions were done, the data plotted to charts of Figures (5.6), (5.7) and (5.8) which shows the relation between the measured discharges versus the discharges that predicted by applying regression Equations to the experimental data.

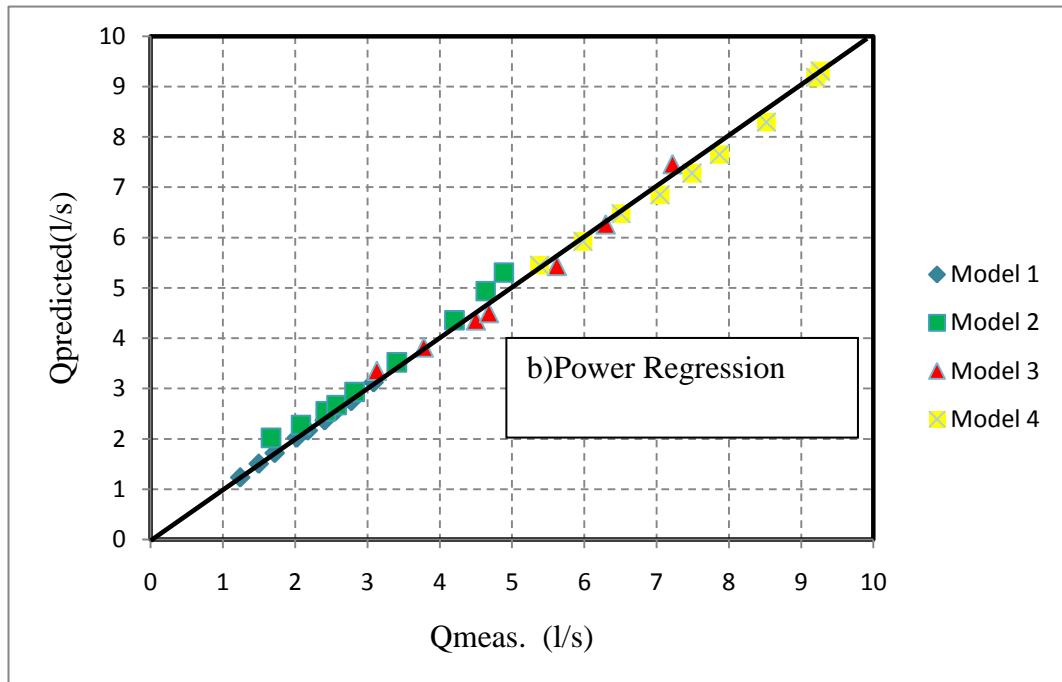
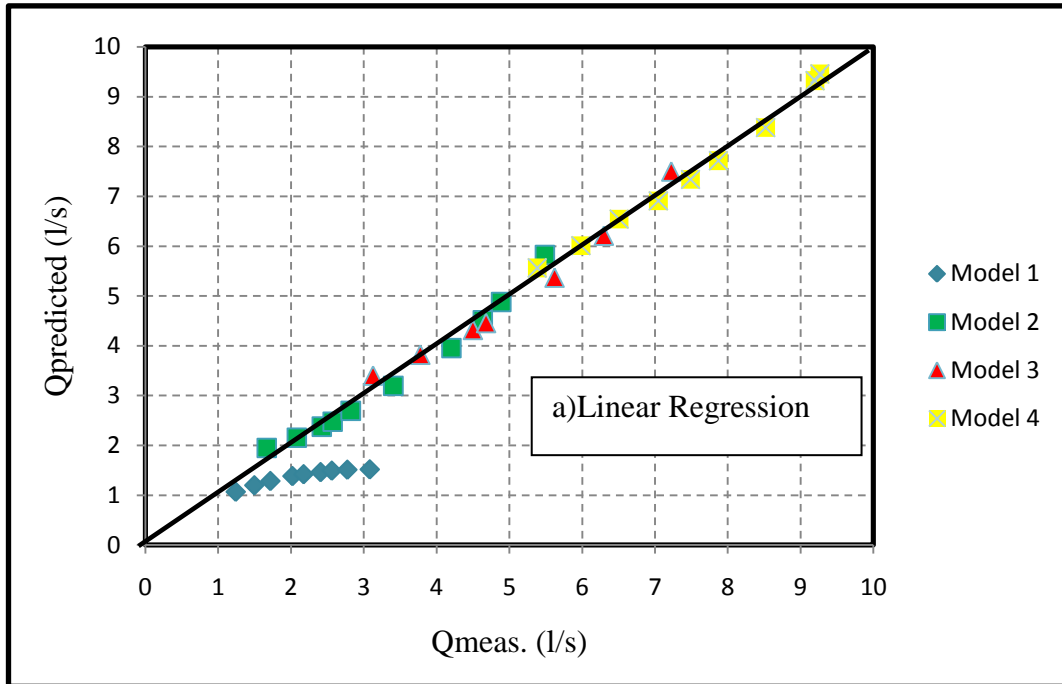


Figure 5.6 Relation between measured and predicted discharges for the culvert
(a)linear regression (b) power regression

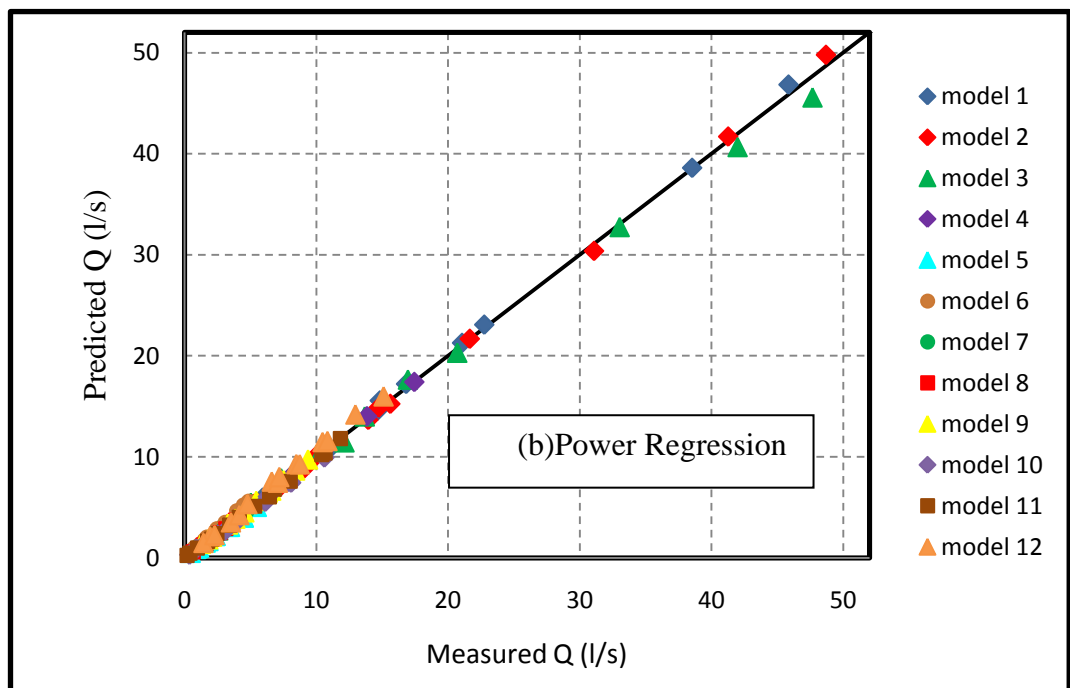
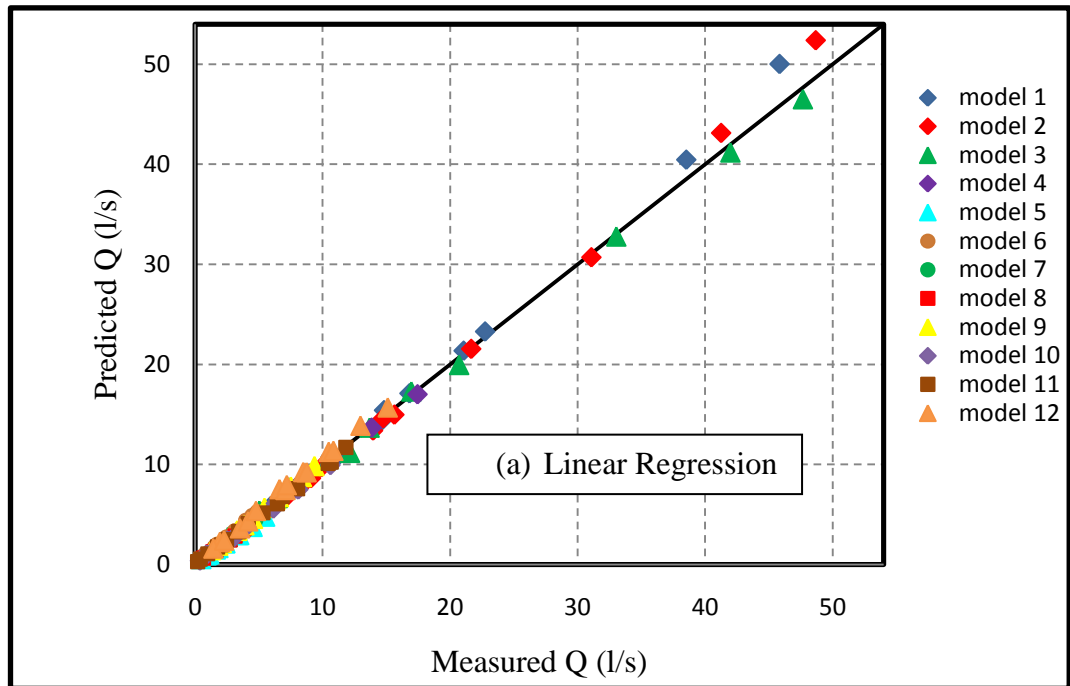


Figure 5.7 Relationship between measured and predicted discharges for the BCW
 (a) Linear regression (b) power regression

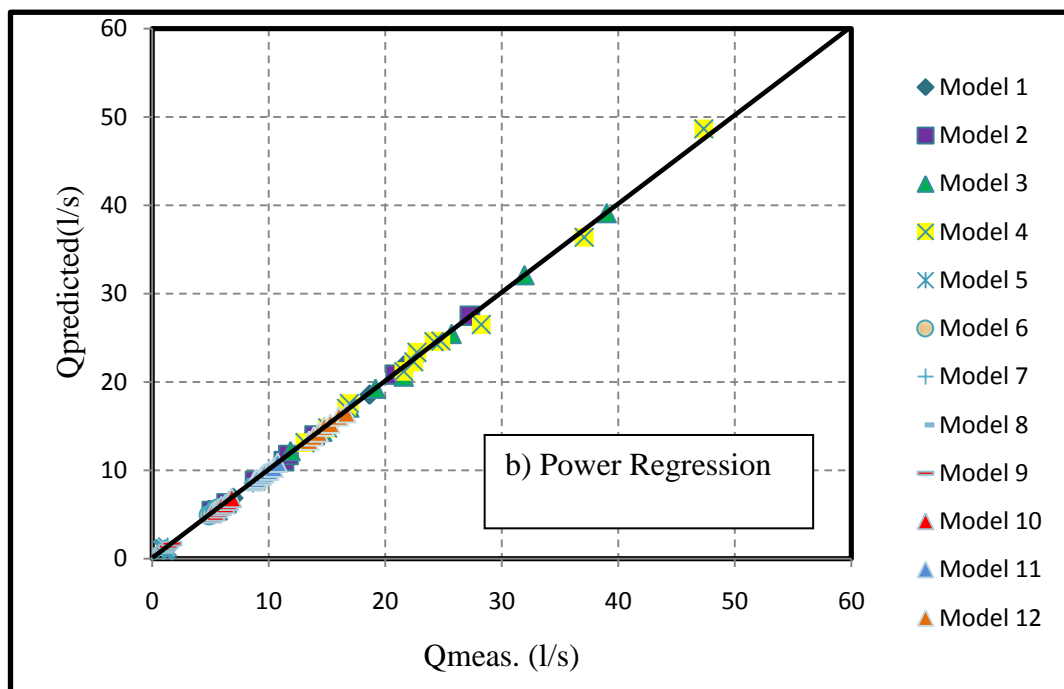
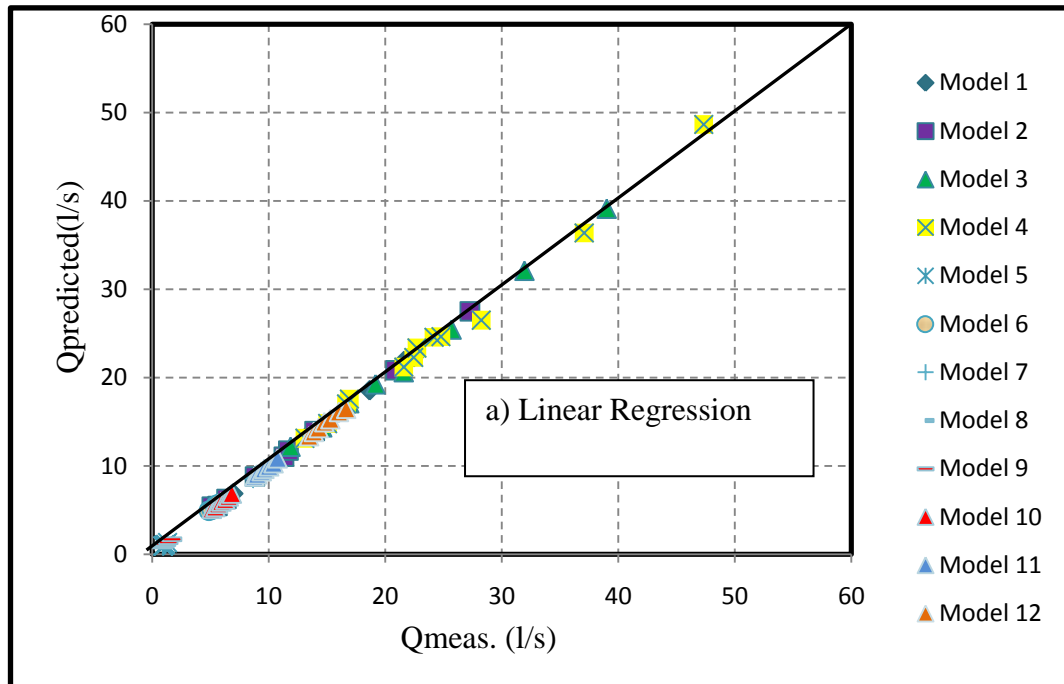


Figure 5.8 Relationship between measured and calculated discharges for the combined structure (a) linear regression (b) power regression

In order to illustrate the variation of discharge coefficients (C_d) with the dimensionless parameters related with it, for each model (C_d) plotted against (H/P), (H/Y), (H/D) and (H/L) as shown in Fig (5.9).

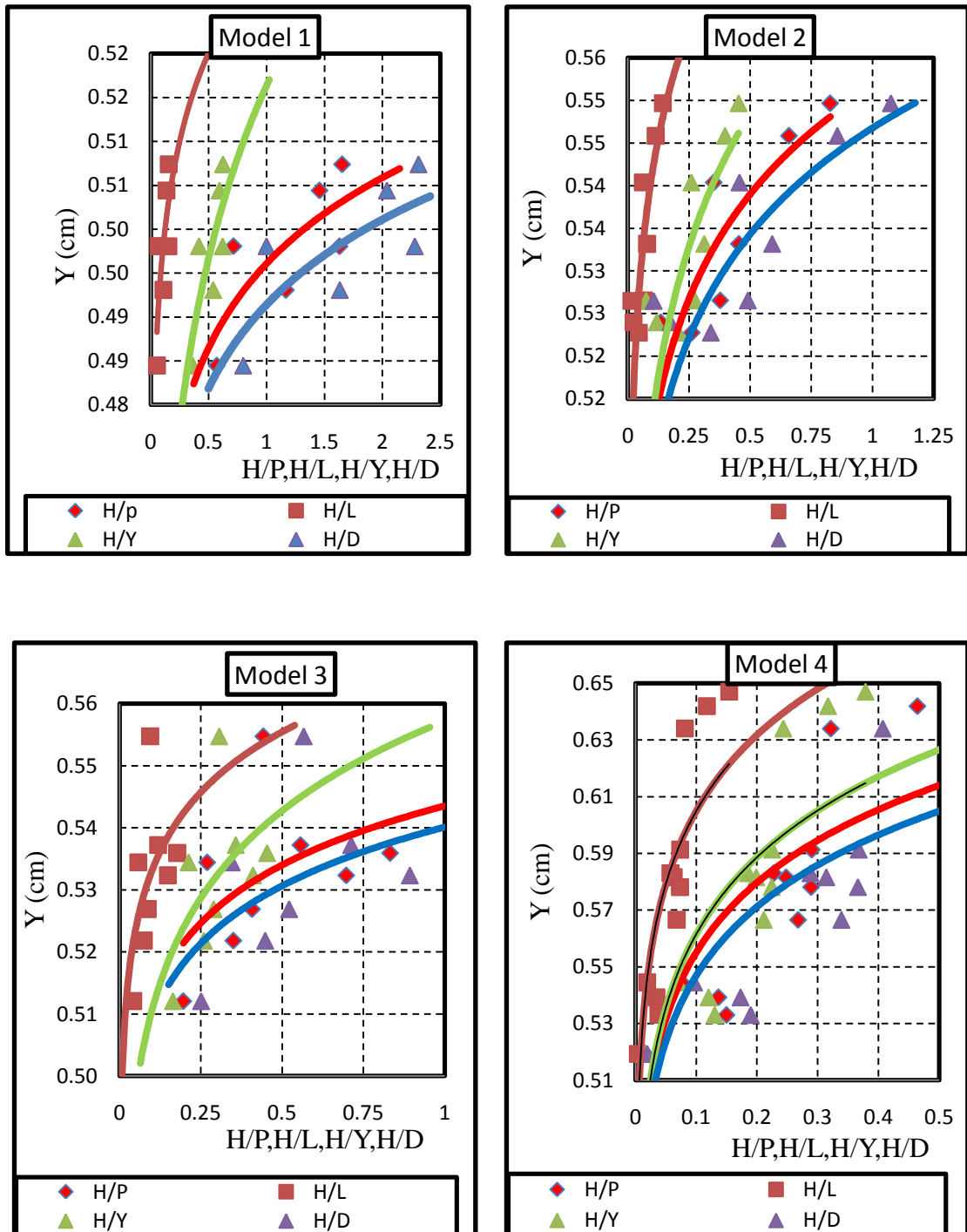


Figure 5.9 Variation of (C_d) with (H/P), (H/Y), (H/D) and (H/L) for models 1-4

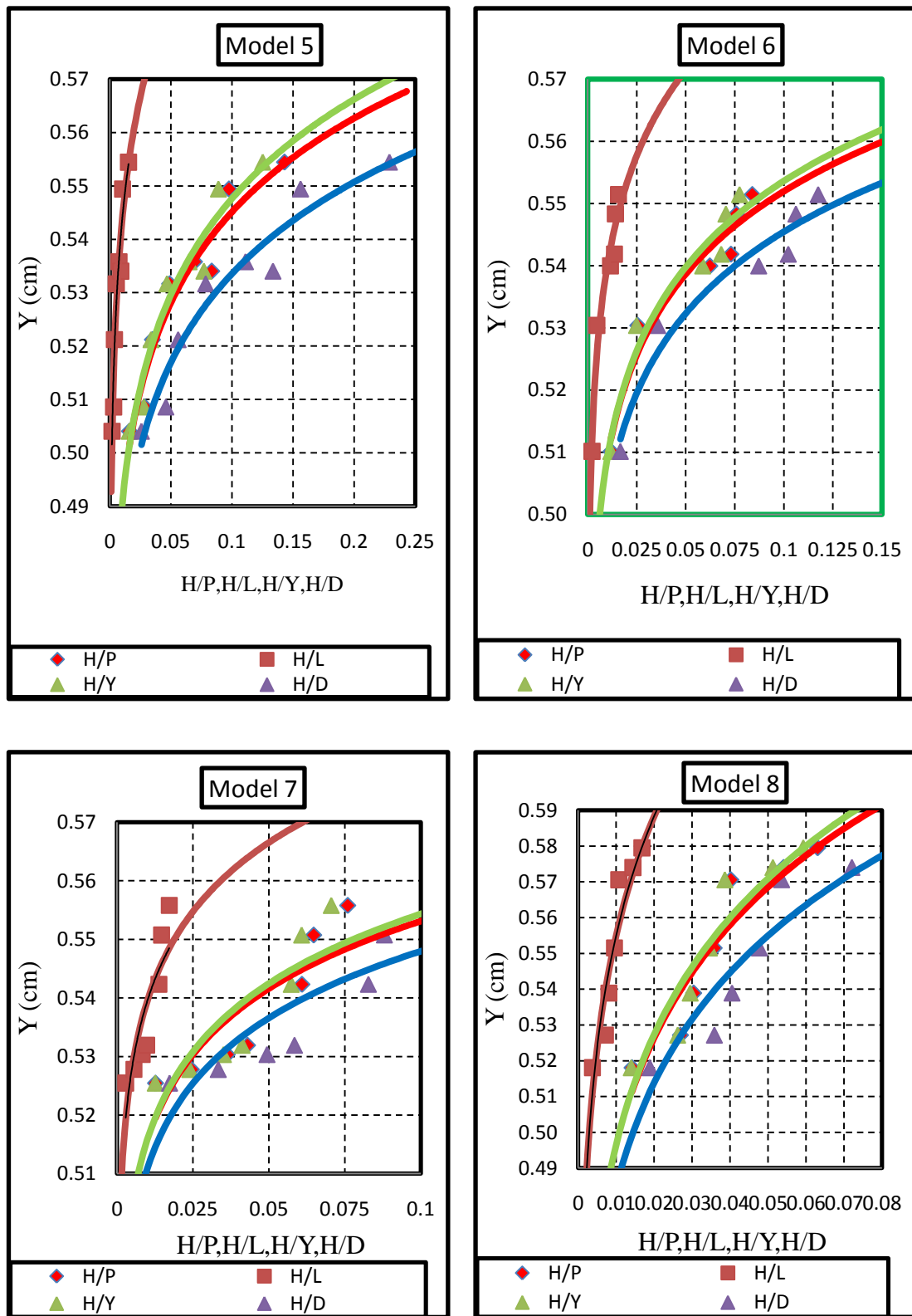


Figure 5.9 Continued, Variation of (Cd) with (H/P), (H/Y), (H/D) and (H/L) for models (5-8)

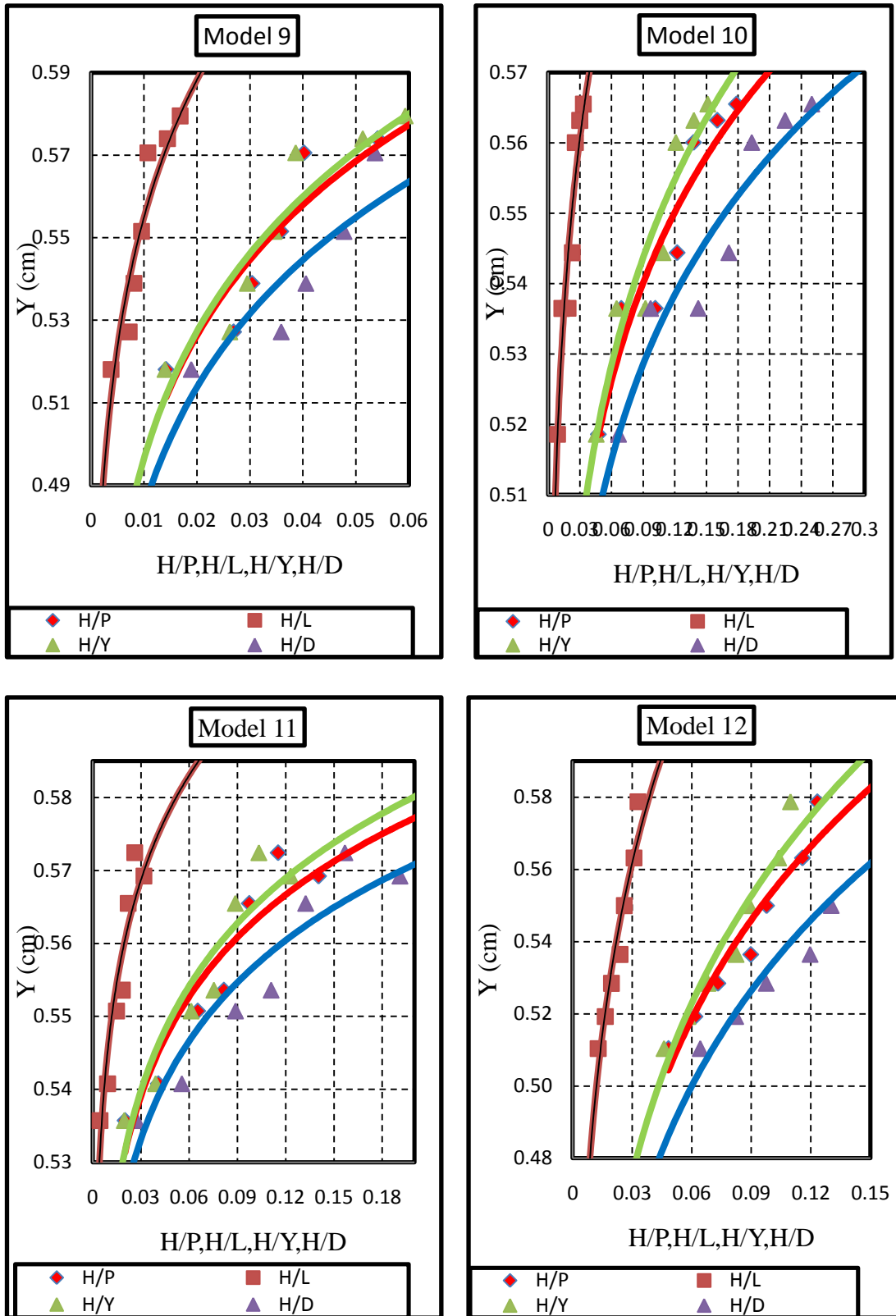


Figure 5.9 Continued, Variation of (Cd) with (H/P), (H/Y), (H/D) and (H/L) for models 9-12

CHAPTER 6

CONCLUSIONS AND RECOMMENDATIONS

6.1 General

In this study, a series of laboratory experiments were conducted in order to investigate the effect of interaction of flow over broad crested weir and box culverts on the discharge coefficient. The effect of the total head of water upstream of the combined structure (Y), the weir crest height (P), the weir crest width (b), angle of weir side slopes (θ), of the broad crested weir and internal dimension of the culvert (D), on the discharge coefficient were studied.

6.2 Conclusions

The following conclusions can be drawn from the analysis of the experimental data of the study:

1. It was observed from Fig (5.1) that for a certain head (Y), combining the discharge through the culvert (Q_c) with the discharge passed over the weir (Q_w) equals to the simultaneous discharge passed through the combined structure (Q_t).
2. The measured discharge (Q) values obtained from the experiments performed on the broad crested weirs has no significant relation with the weir height (P) for each group of models having the same cross section shape and crest length (L) as indicated from Fig (5.2). This conclusion agreed with the results obtained by M. Göğüş, Z. Defne and V. Özkandemir (2006), [20].

3. The value of Coefficient of discharge (C_d) increases as the ratio (H/P) increases for all the tested models and for each flow state (weir and combined) as shown in Fig (5.3) . This conclusion agreed with the results obtained by Amir Hossein Azimi and N. Rajaratnam (2009),[15], Kassem Salah El- Alfy (2005),[19] and Sarhan Abdul star Sarhan (1989),[12].
4. For certain value of the ratio (H/P), the (C_d) value increases with the decreasing of the angle of weirsides (θ), for all the tested models and for each flow state (weir and combined) as shown in Fig (5.3).
5. The value of (C_d) increases as the ratio (Y/D) increase for all the models tested as culvert flow only, this conclusion agreed with results obtained by (Bodhaine, 1976) [7], [27] which has been cleared in Fig (5.4).
6. For a certain upstream water height (Y) the discharge coefficient (C_d) values obtained from the experiments performed on the culvert flow increases with decreasing in the culvert dimension (D), as shown in Fig (5.5).
7. Figures (5.6), (5.7) and (5.8), shows good agreement between the measured and predicted discharges for the tested models.

6.3 Recommendations for further Investigations

The combination of broad crested weirs and culverts still leave areas which require further study. The following items are recommended for further studies:

1. Studying the effect of the flume bed slope on the flow characteristics of the combined structure.
2. Studying the flow characteristics in the case of submerged flow downstream of the combined structure.
3. Studying the flow characteristics through combined broad crested weir and pipe shape culverts.

REFERENCES

- [1] McDonald, T., & Anderson-Wilk, M. (2003). Low Water Stream Crossings in Iowa: A Selection and Design Guide.
- [2] Tuncok, I. K., & Mays, L. W. (2001). Hydraulic Design of culverts and highway structures. *Stormwater Collection Systems Design Handbook*, McGraw-Hill, New York.
- [3] Meselhe, E. A., & Hebert, K. (2007). Laboratory measurements of flow through culverts. *Journal of Hydraulic Engineering*, 133(8), 973-976.
- [4] Chaudhry, M. H. (2007). *Open-channel flow*. Springer Publishing Company, Incorporated.
- [5] Akan, A. O. (2006). *Open channel hydraulics*. Butterworth-Heinemann.
- [6] Chow, V. T. (1959). *Open-channel hydraulics*.
- [7] French, R. H., & French, R. H. (1985). *Open-channel hydraulics*.
- [8] Bos, M. G. (1976). Discharge measurement structures. *NASA STI/Recon Technical Report N*, 78, 31395.
- [9] Subramanya, K. (2009). *Flow in open channels*. Tata McGraw-Hill.
- [10] Novák, P. (2001). *Hydraulic structures*. Taylor & Francis.
- [11] Breusers, H. N. C., & Raudkivi, A. J. (1991). Scouring, hydraulic structures design manual. *IAHR, AA Balkema, Rotterdam*, 143.
- [12] Kandaswamy, P. K., & Rouse, H. (1957). Characteristics of flow over terminal weirs and sills. *Journal of the Hydraulics Division*, 83(4), 1-13.
- [13] Ghanim Mohamad Ibraheem. (1983). "Discharge and Flow Characteristics of Weirs with Triangular Plan Form" M. Sc. Thesis, College of Engineering, University of Mosul.

- [14] Kindsvater, C. E., & Carter, R. W. (1957). Discharge characteristics of rectangular thin-plate weirs. *Journal of the Hydraulics Division*, 83(6), 1-36
- [15] Azimi, A. H., & Rajaratnam, N. (2009). Discharge characteristics of weirs of finite crest length. *Journal of Hydraulic Engineering*, 135(12), 1081-1085.
- [16] Govinda Rao, N. S., & Muralidhar, D. (1963). Discharge characteristics of weirs of finite-crest width. *La Houille Blanche*, (5), 537-545.
- [17] Henderson, F. M. (1966). *Open Channel Flow*, Macmillian, New York.
- [18] A. Khosrojerdi, A., & Kavianpour, M. R. (2002). Hydraulic Behaviour of Straight and Curved Broad Crested Weirs. In *Proc. Fifth International Conference on Hydro-Science and Engineering*.
- [19] El-Alfy, K. S. Effect of Vertical Curvature of Flow at Weir Crest on Discharge Coefficient..
- [20] Göğüş, M., Defne, Z., & Özkandemir, V. (2006). Broad-crested weirs with rectangular compound cross sections. *Journal of irrigation and drainage engineering*, 132(3), 272-280.
- [21] Sargison, J. E., & Percy, A. (2009). Hydraulics of broad-crested weirs with varying side slopes. *Journal of Irrigation and Drainage Engineering*, 135(1), 115-118.
- [22] Ferro, V. (2000). Simultaneous flow over and under a gate. *Journal of irrigation and drainage engineering*, 126(3), 190-193.
- [23] Negm, A. M. (2002). Analysis and modeling of simultaneous flow through box culverts and over contracted broad-crested weirs. In *Proc. of 5th Int. Conf. on Hydro-science and Engineering. ICHE2002. Sept* (pp. 18-21)
- [24] Featherstone, R. E., & Nalluri, C. (1982). *Civil engineering hydraulics: essential theory with worked examples*.
- [25] Chanson, H. (2004). *The hydraulics of open channel flow: an introduction; basic principles, sediment motion, hydraulic modelling, design of hydraulic structures*. Butterworth-Heinemann.
- [26] Webber, N. B. (1965). *Fluid mechanics for civil engineers*. E. & FN Spon.
- [27] Bodhaine, G. L. (1968). *Measurement of peak discharge at culverts by indirect methods*. US Government Printing Office.
- [28] Streeter, V. L., Wylie, E. B., & Bedford, K. W. (1998). *Fluid mechanics*, WCB McGraw-Hill. Inc, Boston, 21..

APPENDICES

Appendix A: Sample of Calculation

Sample of calculation for Model (1), test run (1) as combined structure flow:

From the equation of the V-notch weir for ($h_v=10.2$ cm):

$$Q_{\text{meas.}} = 0.0195(10.2)^{2.398} = 5.09 \text{ l/sec}$$

Approach velocity in the Flume upstream of the test Model (v_o) for ($y_o=9.53$ cm) & width of the Flume ($B=50$ cm):

$$v_o = \frac{Q_{\text{meas.}}}{B * y_o} = \frac{5.09 * 1000}{50 * 9.53} = 10.68 \text{ cm/sec}$$

Approach velocity head in the Flume upstream of the test Model:

$$\frac{v_o^2}{2g} = \frac{(10.68)^2}{2 * 980.6} = 0.06 \text{ cm}$$

Upstream total head of water on the inlet of the culvert (Y):

$$Y = y_o - T + \frac{v_o^2}{2g} = 9.53 - 0.8 + 0.06 = 8.79 \text{ cm}$$

$$Q_c = D * D\sqrt{2gY} = 4 * 4\sqrt{2 * 980.6 * 8.79}/1000 = 2.1 \text{ l/sec.}$$

Upstream total head of water on the weir crest (H):

$$H = Y - P = 8.79 - 5.6 = 3.19 \text{ cm}$$

$$Q_w = \left(\frac{2}{3} \sqrt{2gb} H^{3/2} + \frac{8}{15} \sqrt{2g} H^{5/2} \tan \theta \right) = \left(\frac{2}{3} \sqrt{2(980.6)} (50) (3.19)^{3/2} + 0 \right)$$
$$= 8.4 \text{ l/sec}$$

$$Q_t = Q_w + Q_c = 2.10 + 8.4 = 10.50 \text{ l/sec}$$

$$C_d = \frac{Q_{\text{meas.}}}{Q_t} = \frac{5.09}{10.5} = 0.484$$

Appendix B: Measured Data and Calculated Results.

Table (B-1) Measured and calculated data for combined structure flow

Model 1				D=4*4 cm, b=50 cm								tan $\theta=0$			
h_v cm	Q_{meas} l/sec	y_o cm	v_o cm/sec	$v_o^2/2g$ cm	Y cm	H cm	Q_{wl} l/sec	Q_c l/sec	Q_t l/sec	H/P	H/b	H/L	H/Y	H/D	cd
10.18	5.09	9.53	10.68	0.06	8.79	3.19	8.40	2.10	10.50	0.569	0.064	0.053	0.363	0.797	0.484
11.6	6.96	10.3	13.51	0.09	9.59	3.99	11.78	2.19	13.97	0.713	0.080	0.067	0.416	0.998	0.498
15.2	13.35	12.7	21.02	0.23	12.13	6.53	24.61	2.47	27.07	1.165	0.131	0.109	0.538	1.631	0.493
17.5	18.66	14.2	26.28	0.35	13.75	8.15	34.36	2.63	36.99	1.456	0.163	0.136	0.593	2.038	0.504
18.6	21.59	15.1	28.60	0.42	14.72	9.12	40.64	2.72	43.36	1.628	0.182	0.152	0.619	2.279	0.498
18.9	22.44	15.2	29.52	0.44	14.84	9.24	41.49	2.73	44.22	1.651	0.185	0.154	0.623	2.311	0.507
Model 2				D=8*8 cm, b=50 cm								tan $\theta=0$			
10.2	5.11	11.96	8.55	0.04	11.20	0.80	1.05	9.48	10.53	0.077	0.016	0.013	0.071	0.100	0.485
10.6	5.61	12	9.34	0.04	11.24	0.84	1.15	9.50	10.65	0.081	0.017	0.014	0.075	0.106	0.526
11.2	6.37	12.54	10.16	0.05	11.79	1.39	2.43	9.73	12.16	0.134	0.028	0.023	0.118	0.174	0.524
12.8	8.81	13.83	12.74	0.08	13.11	2.71	6.60	10.26	16.86	0.261	0.054	0.045	0.207	0.339	0.523
14.2	11.30	14.73	15.35	0.12	14.05	3.65	10.29	10.62	20.92	0.351	0.073	0.061	0.260	0.456	0.540
14.4	11.69	15	15.59	0.12	14.32	3.92	11.47	10.73	22.20	0.377	0.078	0.065	0.274	0.490	0.527
15.5	13.95	15.76	17.70	0.16	15.12	4.72	15.14	11.02	26.16	0.454	0.094	0.079	0.312	0.590	0.533
18.3	20.88	17.77	23.50	0.28	17.25	6.85	26.47	11.77	38.25	0.659	0.137	0.114	0.397	0.856	0.546
20.5	27.27	19.4	28.11	0.40	19.00	8.60	37.25	12.36	49.60	0.827	0.172	0.143	0.453	1.075	0.550

Table (B-1) Continued

Model 3				D= 10*10 cm, b=50 cm								tan $\theta=0$			
h_v cm	Q_{meas} l/sec	y_o cm	v_o cm/sec	$v_o^2/2g$ cm	Y cm	H cm	Q_w l/sec	Q_c l/sec	Q_t l/sec	H/P	H/b	H/L	H/Y	H/D	cd
14.5	11.88	16	14.86	0.11	15.31	2.51	5.88	17.33	23.21	0.20	0.05	0.04	0.16	0.25	0.512
15.8	14.60	16.9	17.28	0.15	16.25	3.45	9.47	17.85	27.32	0.27	0.07	0.06	0.21	0.35	0.534
16.8	16.92	17.9	18.9	0.18	17.28	4.48	14.01	18.41	32.42	0.35	0.09	0.07	0.26	0.45	0.522
17.7	19.17	18.6	20.62	0.22	18.02	5.22	17.59	18.80	36.39	0.41	0.10	0.09	0.29	0.52	0.527
18.6	21.59	19	22.73	0.26	18.46	5.66	19.90	19.03	38.92	0.44	0.11	0.09	0.31	0.57	0.555
20	25.70	20.4	25.19	0.32	19.92	7.12	28.07	19.77	47.83	0.56	0.14	0.12	0.36	0.71	0.537
21.9	31.95	22.1	28.91	0.43	21.73	8.93	39.37	20.64	60.01	0.70	0.18	0.15	0.41	0.89	0.532
23.8	39.00	23.7	32.91	0.55	23.45	10.65	51.32	21.45	72.77	0.83	0.21	0.18	0.45	1.07	0.536
Model 4				D= 12*12 cm, b=50 cm								tan $\theta=0$			
15.1	13.10	16.1	16.27	0.13	15.43	0.23	0.17	25.05	25.22	0.015	0.005	0.004	0.015	0.020	0.519
16	15.05	17	17.70	0.16	16.36	1.16	1.84	25.79	27.64	0.076	0.023	0.019	0.071	0.097	0.545
16.7	16.68	17.9	18.63	0.18	17.28	2.08	4.42	26.51	30.93	0.137	0.042	0.035	0.120	0.173	0.539
16.8	16.92	18.1	18.69	0.18	17.48	2.28	5.08	26.66	31.74	0.150	0.046	0.038	0.130	0.190	0.533
18.6	21.59	19.2	22.49	0.26	18.66	3.46	9.49	27.55	37.04	0.227	0.069	0.058	0.185	0.288	0.583
18.9	22.44	19.5	23.01	0.27	18.97	3.77	10.81	27.78	38.58	0.248	0.075	0.063	0.199	0.314	0.582
19	22.72	19.8	22.95	0.27	19.27	4.07	12.11	27.99	40.11	0.268	0.081	0.068	0.211	0.339	0.567
19.5	24.18	20.1	24.06	0.30	19.60	4.40	13.60	28.23	41.83	0.289	0.088	0.073	0.224	0.366	0.578
19.7	24.78	20.1	24.66	0.31	19.61	4.41	13.67	28.24	41.91	0.290	0.088	0.074	0.225	0.368	0.591
20.8	28.23	20.5	27.54	0.39	20.09	4.89	15.95	28.58	44.53	0.322	0.098	0.081	0.243	0.407	0.634
23.3	37.06	22.5	32.95	0.55	22.25	7.05	27.65	30.08	57.74	0.464	0.141	0.118	0.317	0.588	0.642
25.8	47.33	24.5	38.63	0.76	24.46	9.26	41.60	31.54	73.14	0.609	0.185	0.154	0.379	0.772	0.647

Table (B-1) Continued

Model 5				D=4*4 cm, b=10 cm								tan θ =11.43			
h_v cm	Q_{meas} l/sec	y_o cm	v_o cm/sec	$v_o^2/2g$ cm	Y cm	H cm	Q_w l/sec	Q_c l/sec	Q_t l/sec	H/P	H/b	H/L	H/Y	H/D	cd
4.98	0.92	7.3	2.51	0.00	6.50	0.10	0.01	1.81	1.818	0.016	0.010	0.002	0.016	0.026	0.504
5.03	0.94	7.38	2.54	0.00	6.58	0.18	0.03	1.82	1.845	0.029	0.018	0.003	0.028	0.046	0.509
5.1	0.97	7.42	2.61	0.00	6.62	0.22	0.04	1.82	1.861	0.035	0.022	0.004	0.034	0.056	0.521
5.19	1.01	7.51	2.69	0.00	6.71	0.31	0.07	1.84	1.903	0.049	0.031	0.005	0.047	0.078	0.532
5.29	1.06	7.64	2.77	0.00	6.84	0.44	0.12	1.85	1.976	0.069	0.044	0.007	0.065	0.111	0.536
5.35	1.09	7.73	2.81	0.00	6.93	0.53	0.17	1.87	2.037	0.083	0.053	0.009	0.077	0.134	0.534
5.49	1.16	7.82	2.96	0.00	7.02	0.62	0.23	1.88	2.107	0.098	0.062	0.010	0.089	0.156	0.549
5.81	1.33	8.11	3.27	0.01	7.32	0.92	0.48	1.92	2.392	0.143	0.092	0.015	0.125	0.229	0.554
Model 6				D=8*8 cm, b=10 cm								tan θ =11.43			
10	4.88	12.1	8.06	0.03	11.33	0.13	0.02	9.54	9.56	0.012	0.013	0.002	0.012	0.017	0.510
10.2	5.12	12.25	8.37	0.04	11.49	0.29	0.06	9.61	9.66	0.026	0.029	0.005	0.025	0.036	0.530
10.5	5.43	12.66	8.58	0.04	11.90	0.70	0.28	9.78	10.06	0.062	0.070	0.012	0.059	0.087	0.540
10.5	5.53	12.78	8.66	0.04	12.02	0.82	0.38	9.83	10.21	0.073	0.082	0.014	0.068	0.102	0.542
10.6	5.62	12.81	8.77	0.04	12.05	0.85	0.41	9.84	10.25	0.076	0.085	0.014	0.070	0.106	0.548
10.7	5.72	12.9	8.87	0.04	12.14	0.94	0.50	9.88	10.38	0.084	0.094	0.016	0.077	0.118	0.551

Table (B-1) Continued

Model 7				D=10*10 cm, b=10 cm								tan θ =11.43			
h_v cm	Q_{meas} l/sec	y_o cm	v_o cm/sec	$v^2/2g$ cm	Y cm	H cm	Q_w l/sec	Q_c l/sec	Qt l/sec	H/P	H/b	H/L	H/Y	H/D	cd
12.7	8.65	14.5	11.93	0.07	13.77	0.17	0.02	16.43	16.46	0.013	0.017	0.003	0.013	0.017	0.525
12.8	8.76	14.66	11.96	0.07	13.93	0.33	0.07	16.53	16.60	0.024	0.033	0.006	0.024	0.033	0.528
12.9	8.90	14.82	12.01	0.07	14.09	0.49	0.15	16.63	16.77	0.036	0.049	0.008	0.035	0.049	0.530
12.9	8.98	14.91	12.04	0.07	14.18	0.58	0.20	16.68	16.88	0.043	0.058	0.010	0.041	0.058	0.532
13.1	9.33	15.15	12.32	0.08	14.43	0.83	0.39	16.82	17.21	0.061	0.083	0.014	0.057	0.083	0.542
13.2	9.52	15.2	12.53	0.08	14.48	0.88	0.44	16.85	17.29	0.065	0.088	0.015	0.061	0.088	0.551
13.4	9.75	15.35	12.70	0.08	14.63	1.03	0.60	16.94	17.54	0.076	0.103	0.017	0.071	0.103	0.556
Model 8				D=12*12 cm, b=10 cm								tan θ =11.43			
15.2	13.33	16.9	15.77	0.13	16.23	0.23	0.04	25.69	25.73	0.014	0.023	0.004	0.014	0.019	0.518
15.4	13.69	17.1	16.01	0.13	16.43	0.43	0.12	25.85	25.97	0.027	0.043	0.007	0.026	0.036	0.527
15.5	14.03	17.15	16.36	0.14	16.49	0.49	0.14	25.89	26.04	0.030	0.049	0.008	0.030	0.041	0.539
15.7	14.43	17.23	16.74	0.14	16.57	0.57	0.19	25.96	26.16	0.036	0.057	0.010	0.035	0.048	0.552
16	14.98	17.29	17.33	0.15	16.64	0.64	0.24	26.02	26.26	0.040	0.064	0.011	0.039	0.054	0.571
16.1	15.28	17.51	17.45	0.16	16.87	0.87	0.42	26.19	26.61	0.054	0.087	0.014	0.051	0.072	0.574
16.2	15.57	17.65	17.65	0.16	17.01	1.01	0.57	26.30	26.87	0.063	0.101	0.017	0.059	0.084	0.580

Table (B-1) Continued

Model 9				D=4*4 cm, b=10 cm								tan $\theta=7.11$			
h_v cm	Q_{meas} l/sec	y_o cm	v_o cm/sec	$v^2/2g$ cm	Y cm	H cm	Q_w l/sec	Q_c l/sec	Qt l/sec	H/P	H/b	H/L	H/Y	H/D	cd
4.9	0.88	7.51	2.35	0.00	6.71	0.31	0.06	1.84	1.90	0.049	0.031	0.005	0.047	0.078	0.465
4.97	0.91	7.53	2.42	0.00	6.73	0.33	0.07	1.84	1.91	0.052	0.033	0.006	0.049	0.083	0.478
5.11	0.97	7.71	2.53	0.00	6.91	0.51	0.14	1.86	2.00	0.080	0.051	0.009	0.074	0.128	0.487
5.31	1.07	7.92	2.70	0.00	7.12	0.72	0.26	1.89	2.15	0.113	0.072	0.012	0.102	0.181	0.498
5.51	1.17	8.15	2.87	0.00	7.35	0.95	0.42	1.92	2.35	0.149	0.095	0.016	0.130	0.239	0.498
5.91	1.38	8.51	3.25	0.01	7.72	1.32	0.78	1.97	2.75	0.206	0.132	0.022	0.170	0.329	0.503
6.43	1.69	8.92	3.79	0.01	8.13	1.73	1.33	2.02	3.35	0.270	0.173	0.029	0.213	0.432	0.505
Model 10				D=8*8 cm, b=10 cm								tan $\theta=7.11$			
10.2	5.11	12.5	8.18	0.03	11.73	0.53	0.15	9.71	9.86	0.048	0.053	0.009	0.046	0.067	0.519
10.5	5.42	12.74	8.51	0.04	11.98	0.78	0.29	9.81	10.10	0.069	0.078	0.013	0.065	0.097	0.536
10.6	5.66	13.1	8.64	0.04	12.34	1.14	0.59	9.96	10.55	0.102	0.114	0.019	0.092	0.142	0.536
10.9	5.93	13.33	8.90	0.04	12.57	1.37	0.84	10.05	10.89	0.122	0.137	0.023	0.109	0.171	0.544
11.1	6.26	13.5	9.28	0.04	12.74	1.54	1.06	10.12	11.18	0.138	0.154	0.026	0.121	0.193	0.560
11.3	6.56	13.75	9.55	0.05	13.00	1.80	1.44	10.22	11.66	0.160	0.180	0.030	0.138	0.225	0.563
11.5	6.83	13.95	9.79	0.05	13.20	2.00	1.78	10.30	12.08	0.178	0.200	0.033	0.151	0.250	0.565

Table (B-1) Continued

Model 11				D=10*10 cm, b=10 cm								tan $\theta=7.11$			
h_v cm	Q_{meas} l/sec	y_o cm	v_o cm/sec	$v_o^2/2g$ cm	Y cm	H cm	Q_w l/sec	Q_c l/sec	Q_t l/sec	H/P	H/b	H/L	H/Y	H/D	cd
12.8	8.78	14.6	12.03	0.07	13.87	0.27	0.05	16.50	16.54	0.020	0.027	0.005	0.020	0.027	0.531
12.9	9.01	14.88	12.11	0.07	14.15	0.55	0.16	16.66	16.82	0.041	0.055	0.009	0.039	0.055	0.536
13.2	9.40	15.21	12.36	0.08	14.49	0.89	0.37	16.86	17.23	0.065	0.089	0.015	0.061	0.089	0.546
13.3	9.63	15.43	12.48	0.08	14.71	1.11	0.56	16.98	17.55	0.082	0.111	0.018	0.075	0.111	0.549
13.5	10.03	15.64	12.83	0.08	14.92	1.32	0.79	17.11	17.90	0.097	0.132	0.022	0.089	0.132	0.561
13.7	10.41	15.88	13.11	0.09	15.17	1.57	1.10	17.25	18.34	0.115	0.157	0.026	0.103	0.157	0.567
13.9	10.76	16.22	13.27	0.09	15.51	1.91	1.63	17.44	19.07	0.140	0.191	0.032	0.123	0.191	0.564
Model 12				D=12*12 cm, b=10 cm								tan $\theta=7.11$			
15.3	13.48	17.45	15.45	0.12	16.77	0.77	0.29	26.12	26.40	0.048	0.077	0.013	0.046	0.064	0.510
15.5	13.88	17.66	15.72	0.13	16.99	0.99	0.45	26.28	26.73	0.062	0.099	0.016	0.058	0.082	0.519
15.7	14.29	17.84	16.02	0.13	17.17	1.17	0.62	26.43	27.05	0.073	0.117	0.020	0.068	0.098	0.528
15.9	14.78	18.1	16.33	0.14	17.44	1.44	0.92	26.63	27.55	0.090	0.144	0.024	0.082	0.120	0.536
16.1	15.30	18.22	16.79	0.14	17.56	1.56	1.09	26.73	27.82	0.098	0.156	0.026	0.089	0.130	0.550
16.4	16.04	18.5	17.34	0.15	17.85	1.85	1.53	26.95	28.48	0.116	0.185	0.031	0.104	0.154	0.563
16.7	16.65	18.61	17.90	0.16	17.97	1.97	1.74	27.04	28.77	0.123	0.197	0.033	0.110	0.164	0.579

Table (B-2) Measured and calculated data for the Broad Crested Weir flow

Model 1				P=5.6 cm,b=50 cm					tan $\theta=0$		
h_v cm	Q_{meas} l/sec	y_o cm	v_o cm/sec	$v^2/2g$ cm	Y cm	H cm	Q_w l/sec	H/P	H/b	H/L	Cd
11	6.13	11.4	10.75	0.06	10.66	4.26	12.97	0.67	0.09	0.07	0.472
12.6	8.49	12.5	13.58	0.09	11.79	5.39	18.49	0.84	0.11	0.09	0.459
15	12.85	14.01	18.34	0.17	13.38	6.98	27.23	1.09	0.14	0.12	0.472
16.1	15.28	14.7	20.78	0.22	14.12	7.72	31.67	1.21	0.15	0.13	0.482
17.6	18.91	15.75	24.02	0.29	15.24	8.84	38.83	1.38	0.18	0.15	0.487
18	19.96	15.9	25.11	0.32	15.42	9.02	40.00	1.41	0.18	0.15	0.499
21.1	29.25	18.05	32.41	0.54	17.79	11.39	56.71	1.78	0.23	0.19	0.516
Model 2				P=9.6 cm, b=50 cm					tan $\theta=0$		
10.7	5.68	16.4	6.93	0.02	15.62	4.42	13.74	0.40	0.09	0.07	0.414
11.3	6.55	16.8	7.80	0.03	16.03	4.83	15.67	0.43	0.10	0.08	0.418
11.7	7.05	17	8.29	0.04	16.24	5.04	16.68	0.45	0.10	0.08	0.423
13.9	10.70	18.45	11.60	0.07	17.72	6.52	24.57	0.58	0.13	0.11	0.436
15.8	14.69	19.56	15.02	0.12	18.88	7.68	31.39	0.69	0.15	0.13	0.468
17.3	18.17	20.65	17.60	0.16	20.01	8.81	38.59	0.79	0.18	0.15	0.471
18.9	22.32	21.52	20.75	0.22	20.94	9.74	44.87	0.87	0.19	0.16	0.498
20.4	27.07	22.69	23.87	0.29	22.18	10.98	53.71	0.98	0.22	0.18	0.504
21.8	31.49	23.25	27.09	0.37	22.82	11.62	58.50	1.04	0.23	0.19	0.538
23.2	36.72	24.35	30.16	0.46	24.01	12.81	67.71	1.14	0.26	0.21	0.542

Table (B-2) Continued

Model 3				P=11.6 cm, b=50 cm					tan $\theta=0$		
h_v cm	Q_{meas} l/sec	y_o cm	v_o cm/sec	$v^2/2g$ cm	Y cm	H cm	Q_w l/sec	H/P	H/b	H/L	Cd
3	0.27	14.99	0.36	0.00	14.19	0.59	0.67	0.04	0.01	0.01	0.406
8.6	3.40	17.52	3.88	0.01	16.73	3.13	8.17	0.23	0.06	0.05	0.416
11.5	6.82	19.24	7.09	0.03	18.47	4.87	15.84	0.36	0.10	0.08	0.430
13.6	10.10	20.62	9.80	0.05	19.87	6.27	23.17	0.46	0.13	0.10	0.436
14.7	12.20	21.3	11.46	0.07	20.57	6.97	27.15	0.51	0.14	0.12	0.449
16.1	15.32	22.12	13.85	0.10	21.42	7.82	32.27	0.57	0.16	0.13	0.475
18	19.96	23.21	17.20	0.15	22.56	8.96	39.60	0.66	0.18	0.15	0.504
19.2	23.27	23.91	19.47	0.19	23.30	9.70	44.62	0.71	0.19	0.16	0.522
22	32.30	25.64	25.19	0.32	25.16	11.56	58.05	0.85	0.23	0.19	0.556
23.4	37.60	27.2	27.65	0.39	26.79	13.19	70.71	0.97	0.26	0.22	0.532
Model 4				P=13.6 cm, b=50 cm					tan $\theta=0$		
11.2	6.41	21.5	5.96	0.02	20.72	4.72	15.13	0.29	0.09	0.08	0.424
13	9.15	22.52	8.12	0.03	21.75	5.75	20.37	0.36	0.12	0.10	0.449
15.1	13.10	23.84	10.99	0.06	23.10	7.10	27.94	0.44	0.14	0.12	0.469
16.8	16.87	24.88	13.56	0.09	24.17	8.17	34.50	0.51	0.16	0.14	0.489
18.8	22.18	26.34	16.84	0.14	25.68	9.68	44.49	0.61	0.19	0.16	0.499
20.8	28.10	27.48	20.45	0.21	26.89	10.89	53.07	0.68	0.22	0.18	0.530

Table (B-2) Continued

Model 5				P=5.6cm, b=10 cm					tan θ =11.43		
h_v cm	Q_{meas} l/sec	y_o cm	v_o cm/sec	$v^2/2g$ cm	Y cm	H cm	Q_w l/sec	H/P	H/b	H/L	Cd
0.7	0.01	7.35	0.02	0.00	6.55	0.15	0.02	0.02	0.02	0.00	0.425
0.94	0.02	7.42	0.05	0.00	6.62	0.22	0.04	0.03	0.02	0.00	0.459
1.2	0.03	7.51	0.08	0.00	6.71	0.31	0.07	0.05	0.03	0.01	0.462
1.61	0.06	7.65	0.16	0.00	6.85	0.45	0.13	0.07	0.05	0.01	0.486
1.8	0.08	7.72	0.21	0.00	6.92	0.52	0.16	0.08	0.05	0.01	0.489
2.1	0.12	7.83	0.30	0.00	7.03	0.63	0.23	0.10	0.06	0.01	0.496
2.82	0.23	8.11	0.58	0.00	7.31	0.91	0.47	0.14	0.09	0.02	0.499
Model 6				P=9.6 cm, b=50 cm					tan θ =11.43		
0.86	0.01	12.2	0.02	0.00	11.40	0.20	0.03	0.02	0.02	0.00	0.435
1.28	0.04	12.35	0.06	0.00	11.55	0.35	0.08	0.03	0.04	0.01	0.437
1.53	0.05	12.44	0.09	0.00	11.64	0.44	0.12	0.04	0.04	0.01	0.447
1.85	0.09	12.56	0.14	0.00	11.76	0.56	0.19	0.05	0.06	0.01	0.456
2.15	0.12	12.67	0.19	0.00	11.87	0.67	0.26	0.06	0.07	0.01	0.468
2.54	0.18	12.82	0.28	0.00	12.02	0.82	0.38	0.07	0.08	0.01	0.475
2.78	0.23	12.91	0.35	0.00	12.11	0.91	0.47	0.08	0.09	0.02	0.482

Table (B-2) Continued

Model 7				P=11.6 cm, b=10 cm					tan θ =11.43		
h_v cm	Q_{meas} l/sec	y_o cm	v_o cm/sec	$v^2/2g$ cm	Y cm	H cm	Q_w l/sec	H/P	H/b	H/L	Cd
0.6	0.01	14.52	0.01	0.00	13.72	0.12	0.01	0.01	0.01	0.00	0.421
1.03	0.02	14.66	0.03	0.00	13.86	0.26	0.05	0.02	0.03	0.00	0.432
1.21	0.03	14.72	0.04	0.00	13.92	0.32	0.07	0.02	0.03	0.01	0.446
1.53	0.05	14.83	0.07	0.00	14.03	0.43	0.12	0.03	0.04	0.01	0.466
1.9	0.09	14.97	0.12	0.00	14.17	0.57	0.19	0.04	0.06	0.01	0.470
2.28	0.14	15.11	0.19	0.00	14.31	0.71	0.29	0.05	0.07	0.01	0.483
2.70	0.21	15.25	0.28	0.00	14.45	0.85	0.41	0.06	0.09	0.01	0.513
Model 8				P=13.6 cm, b=10 cm					tan θ =11.43		
1.41	0.04	17.2	0.05	0.00	16.40	0.40	0.10	0.03	0.04	0.01	0.436
1.82	0.08	17.35	0.09	0.00	16.55	0.55	0.18	0.03	0.06	0.01	0.453
2.03	0.11	17.44	0.12	0.00	16.64	0.64	0.24	0.04	0.06	0.01	0.445
2.36	0.15	17.56	0.17	0.00	16.76	0.76	0.33	0.05	0.08	0.01	0.461
2.5	0.18	17.61	0.20	0.00	16.81	0.81	0.37	0.05	0.08	0.01	0.468
2.8	0.23	17.7	0.26	0.00	16.90	0.90	0.46	0.06	0.09	0.02	0.501
3.01	0.27	17.73	0.31	0.00	16.93	0.93	0.49	0.06	0.09	0.02	0.559

Table (B-2) Continued

Model 9				P=5.6 cm, b=10 cm					tan $\theta=7.11$		
h_v cm	Q_{meas} l/sec	y_o cm	v_o cm/sec	$v_o^2/2g$ cm	Y cm	H cm	Q_w l/sec	H/P	H/b	H/L	Cd
0.65	0.01	7.33	0.02	0.00	6.53	0.13	0.01	0.02	0.01	0.00	0.467
1.23	0.03	7.54	0.08	0.00	6.74	0.34	0.07	0.05	0.03	0.01	0.459
1.79	0.08	7.77	0.20	0.00	6.97	0.57	0.17	0.09	0.06	0.01	0.468
2.56	0.19	8.10	0.46	0.00	7.30	0.90	0.38	0.14	0.09	0.02	0.487
3.48	0.39	8.52	0.91	0.00	7.72	1.32	0.78	0.21	0.13	0.02	0.495
4.1	0.57	8.83	1.30	0.00	8.03	1.63	1.19	0.25	0.16	0.03	0.485
4.77	0.83	9.10	1.82	0.00	8.30	1.90	1.61	0.30	0.19	0.03	0.513
Model 10				P=9.6 cm, b=10 cm					tan $\theta=7.11$		
1.57	0.06	12.50	0.09	0.00	11.70	0.50	0.13	0.04	0.05	0.01	0.429
2.17	0.12	12.77	0.20	0.00	11.97	0.77	0.29	0.07	0.08	0.01	0.436
2.58	0.19	12.95	0.29	0.00	12.15	0.95	0.42	0.08	0.10	0.02	0.449
3.15	0.31	13.21	0.46	0.00	12.41	1.21	0.66	0.11	0.12	0.02	0.460
3.89	0.51	13.56	0.75	0.00	12.76	1.56	1.09	0.14	0.16	0.03	0.467
4.27	0.63	13.71	0.92	0.00	12.91	1.71	1.30	0.15	0.17	0.03	0.486
4.68	0.79	13.88	1.14	0.00	13.08	1.88	1.58	0.17	0.19	0.03	0.501
4.95	0.90	14.00	1.29	0.00	13.20	2.00	1.79	0.18	0.20	0.03	0.505

Table (B-2) Continued

Model 11				P=11.6 cm, b=10 cm					tan θ =7.11		
h_v cm	Q_{meas} l/sec	y_o cm	v_o cm/sec	$v^2/2g$ cm	Y cm	H cm	Q_w l/sec	H/P	H/b	H/L	Cd
0.95	0.02	14.65	0.02	0.00	13.85	0.25	0.04	0.02	0.03	0.00	0.409
1.4	0.04	14.83	0.06	0.00	14.03	0.43	0.10	0.03	0.04	0.01	0.422
1.86	0.09	15.01	0.12	0.00	14.21	0.61	0.19	0.04	0.06	0.01	0.456
2.37	0.15	15.22	0.20	0.00	14.42	0.82	0.32	0.06	0.08	0.01	0.480
2.66	0.20	15.33	0.27	0.00	14.53	0.93	0.40	0.07	0.09	0.02	0.503
3.8	0.48	15.84	0.60	0.00	15.04	1.44	0.93	0.11	0.14	0.02	0.516
4.4	0.68	16.11	0.85	0.00	15.31	1.71	1.30	0.13	0.17	0.03	0.523
4.78	0.83	16.27	1.02	0.00	15.47	1.87	1.56	0.14	0.19	0.03	0.533
Model 12				P=13.6 cm, b=10 cm					tan θ =7.11		
1.61	0.06	17.32	0.07	0.00	16.52	0.52	0.14	0.03	0.05	0.01	0.426
2.3	0.14	17.61	0.16	0.00	16.81	0.81	0.31	0.05	0.08	0.01	0.457
2.8	0.23	17.84	0.26	0.00	17.04	1.04	0.50	0.07	0.10	0.02	0.462
3.23	0.32	18.01	0.36	0.00	17.21	1.21	0.66	0.08	0.12	0.02	0.489
3.74	0.46	18.25	0.51	0.00	17.45	1.45	0.94	0.09	0.15	0.02	0.490
4.41	0.68	18.56	0.74	0.00	17.76	1.76	1.38	0.11	0.18	0.03	0.496
4.8	0.84	18.71	0.90	0.00	17.91	1.91	1.63	0.12	0.19	0.03	0.516
5.1	0.97	18.8	1.03	0.00	18.00	2.00	1.79	0.13	0.20	0.03	0.543

Table (B-3) Measured and calculated data for the Culvert flow

Model 1					D=4 cm				
h_v cm	Q_{meas} l/sec	y_o cm	v_o cm/sec	$v^2/2g$ cm	Y cm	Q_c l/sec	Y/L	Y/D	cd
5.65	1.24	9.63	2.58	0.00	9.23	2.15	0.15	2.308	0.576
6.11	1.50	12.86	2.33	0.00	12.46	2.50	0.21	3.116	0.598
6.47	1.72	15.6	2.20	0.00	15.20	2.76	0.25	3.801	0.621
6.925	2.02	19.83	2.04	0.00	19.43	3.12	0.32	4.858	0.647
7.14	2.17	21.93	1.98	0.00	21.53	3.29	0.36	5.383	0.661
7.45	2.41	25.03	1.92	0.00	24.63	3.52	0.41	6.158	0.684
7.645	2.56	28.07	1.82	0.00	27.67	3.73	0.46	6.918	0.687
7.905	2.77	31.28	1.77	0.00	30.88	3.94	0.51	7.720	0.705
8.26	3.08	37.79	1.63	0.00	37.39	4.33	0.62	9.348	0.712
Model 2					D=8 cm				
6.39	1.67	8.45	3.94	0.01	8.06	8.05	0.13	1.007	0.207
7.01	2.08	9.89	4.21	0.01	9.50	8.74	0.16	1.187	0.238
7.47	2.42	11.46	4.23	0.01	11.07	9.43	0.18	1.384	0.257
7.66	2.57	12.19	4.22	0.01	11.80	9.74	0.20	1.475	0.264
7.96	2.82	13.79	4.09	0.01	13.40	10.37	0.22	1.675	0.272
8.61	3.41	17.6	3.87	0.01	17.21	11.76	0.29	2.151	0.290
9.4	4.20	23.42	3.59	0.01	23.03	13.60	0.38	2.878	0.309
9.79	4.63	27.68	3.35	0.01	27.29	14.81	0.45	3.411	0.313
10.01	4.89	30.5	3.20	0.01	30.11	15.55	0.50	3.763	0.314
10.505	5.49	37.59	2.92	0.00	37.19	17.29	0.62	4.649	0.317

Table (B-3) Continued

Model 3					D=10 cm				
h_v cm	Q_{meas} l/sec	y_o cm	v_o cm/sec	$v^2/2g$ cm	Y cm	Q_c l/sec	Y/L	Y/D	cd
8.31	3.13	11.33	5.52	0.02	10.95	14.65	0.18	1.095	0.213
8.99	3.78	12.98	5.82	0.02	12.60	15.72	0.21	1.260	0.240
9.67	4.50	14.91	6.03	0.02	14.53	16.88	0.24	1.453	0.267
9.83	4.68	15.44	6.06	0.02	15.06	17.19	0.25	1.506	0.272
10.61	5.62	18.87	5.96	0.02	18.49	19.04	0.31	1.849	0.295
11.125	6.30	21.93	5.74	0.02	21.55	20.56	0.36	2.155	0.306
11.78	7.22	26.43	5.46	0.02	26.05	22.60	0.43	2.605	0.320
Model 4					D=12 cm				
10.42	5.38	12.98	8.29	0.04	12.62	22.65	0.21	1.051	0.238
10.89	5.98	14.12	8.47	0.04	13.76	23.65	0.23	1.146	0.253
11.28	6.51	15.45	8.43	0.04	15.09	24.77	0.25	1.257	0.263
11.66	7.05	16.36	8.61	0.04	16.00	25.51	0.27	1.333	0.276
11.96	7.49	17.41	8.60	0.04	17.05	26.33	0.28	1.421	0.284
12.21	7.87	18.31	8.60	0.04	17.95	27.02	0.30	1.496	0.291
12.62	8.52	19.89	8.57	0.04	19.53	28.18	0.33	1.627	0.302
13.03	9.20	22.07	8.33	0.04	21.71	29.71	0.36	1.809	0.310
13.07	9.27	22.38	8.28	0.03	22.01	29.92	0.37	1.835	0.310